Hindawi
Adsorption Science & Technology
Volume 2022, Article ID 5820207, 25 pages
https://doi.org/10.1155/2022/5820207

Research Article

Chemical Modification of *Teff* Straw Biomass for Adsorptive Removal of Cr (VI) from Aqueous Solution: Characterization, Optimization, Kinetics, and Thermodynamic Aspects

Ashagrie Liyew Ayele,[1] Belachew Zegale Tizazu ,[1] and Abrham Bayeh Wassie[2]

[1]*Department of Chemical Engineering, Addis Ababa Science and Technology University, Addis Ababa, Ethiopia*
[2]*Department of Chemical Engineering, University of Gondar, Ethiopia*

Correspondence should be addressed to Belachew Zegale Tizazu; belachew.zegale@aastu.edu.et

Received 30 August 2021; Accepted 28 March 2022; Published 15 April 2022

Academic Editor: Daniel Schwantes

Teff straw, a by-product of *Teff*, mainly available in Ethiopia, has not been studied much for biosorbent production. The present study has investigated the effects of modification and optimization of process parameters (viz., concentration of modifying agent (H_3PO_4 and KOH), modifying temperature, and modifying time) on the Cr (VI) removal efficiency of using chemically activated *Teff* straw biosorbent by RSM followed by BBD. The maximum Cr (VI) removal was obtained using an H_3PO_4-modified *Teff* straw biosorbent of 92.5% with 2 M concentration of the modifying agent, 110°C, and 4 h. Similarly, maximum Cr (VI) removal using KOH-modified *Teff* straw biosorbent of 95.2% was obtained with 1.5 M activating agent concentration, 105°C activation temperature, and 3.5 h activation time. In addition, the effects of adsorption parameters (viz., biosorbent dosage, temperature, initial concentration of Cr (VI), and contact time) were investigated. The maximum removal efficiency was attained at 2 g of biosorbent dosage, 4 h contact, 75 mg/L of initial Cr (VI) concentration, and 25°C sorption temperature. In addition, isotherm, kinetic, and thermodynamic studies for Cr (VI) biosorption were studied. The experimental adsorption data were well fitted with the Langmuir isotherm and pseudo-second-order kinetic model with higher correlation coefficient in both untreated and chemically modified *Teff* straw biosorbent. The investigated thermodynamic parameters (ΔH^o, ΔS^o, and ΔG^o) confirmed that Cr (VI) metal ions' adsorption process onto Teff straw biosorbent was spontaneous and endothermic.

1. Introduction

The frequent utilization of fossil-based products becomes a significant cause of economic breakdown and environmental degradation. Therefore, alternative, cost-effective, abundant, environmental-friendly, and biorenewable feedstocks must be investigated [1, 2].

Lignocellulosic biomass is a typically nonedible material mainly deduced from woody biomass, nonwoody biomass, and organic wastes. In the last few decades, interests have been grown almost in all developed, developing, and underdeveloped countries for the utilization of lignocellulosic biomass for various economic sectors, namely, renewable energy, dispersants, biocomposites, fertilizer, textile, pharmaceuticals, adsorbents, additives, phenolic compounds, and food industry [3, 4]. However, due to rapid industrial development, discharges of pollutants such as heavy metals to the environment through wastewater have remarkably been increased. Thus, environmental pollution with heavy metals is a serious issue worldwide, posing threats to humans, animals, and plants and the overall ecosystem's stability [5, 6].

In the industrial wastewater treatment sector, heavy metals such as chromium, copper, cadmium, lead, zinc, and nickel are considered more toxic and receive more researchers' attention. Chromium (Cr) is a harmful heavy metal and exists in various oxidative forms. Cr (VI) is considered more harmful and toxic due to its high carcinogenic and resistant properties than Cr (III) [7, 8]. Various Cr contamination sources include electroplating, leather tanning, textile industries, metal finishing, nuclear power plants,

and chromate preparation. Effluents from tannery industries are among the problematic environmental issues faced by the Ethiopian manufacturing sector. Tannery effluents have been reported to contain a high amount of heavy metals such as chromium and organic pollutants [1, 2, 8].

In developing countries, 70% of industrial effluents are discharged into the environment without any treatment action. Industries that contribute as a source for such effluents are the processing of radioactive materials, the manufacture of electrical equipment, electroplating, leather tanning, metal finishing, dyes and pigments, mining operations, fossil fuel combustion, metallurgical operations, mineral processing, fly ash from incinerators, refining ores, pesticides, and preservative [8, 9]. The increasing levels of toxic and hazardous heavy metals that interfere with the biosphere cause immediate economic crisis and hazardous health effects.

To date, researchers have focused on investigating cheap and readily available biomass as a source of biosorbent instead of using very expensive, nonrenewable, non-eco-friendly, nonbiodegradable, and continually depleted fossil sources [7, 10]. Synthetic adsorbents like zeolites, silica gel, alumina, concrete, and polymers also have high production costs and less adsorption capacity than biosorbents obtained from biomass sources [11, 12]. Various researchers have given special attention to biosorbents from agricultural and industrial residue due to high porosity and their availability in large quantities at low cost [1, 2, 13].

Biosorbents prepared from lignocellulosic biomass could be promising materials to remove various toxic, hazardous, and nonbiodegradable organic and inorganic pollutants such as heavy metals, recovery of high-value proteins, specific organic compounds (phenolic compounds, polycyclic aromatic hydrocarbons, organic pesticides, and herbicides agrochemicals), dissolved compounds, and suspended solids of water from the effluents of various industries [10, 14, 15]. Biosorption has been more feasible, economical, simple, and advantageous over the well-known conventional techniques enclosed phytoremediation, ultrafiltration, ion exchange, reverse osmosis, electrodialysis, chemical precipitation, and electrochemical oxidation [12, 16]. Various authors have addressed the biosorption process which provided various advantages: low operating cost, readily available, high adsorption capacity, minimum chemical and/or biological sludge, no additional nutrient requirements, regeneration of biosorbent and the possibility of metal recovery, and short operation time and improved selectivity for specific metals of interest. However, the commercial treatment methods are less effective and more expensive in capital and operational costs [17–20].

In Ethiopia, various potential agricultural/industrial waste sources are unlimited [18, 21]. Among the many biomass wastes, *Teff* straw is one of the abundantly available, feasible, and locally sourced materials for synthesizing low-cost biosorbent. Various researchers have shown that adsorbents obtained from various agricultural wastes, such as *Teff* straw, have been widely used to remove different toxic heavy metals from wastewater. Characterization and utilization *Teff* straw for chromium removal from wastewater, viz., kinetics, isotherm, and thermodynamic modeling, have been reported by Wassie and Srivastava [22]. Wassie and Srivastava [23] have also studied the chemical modification of *Teff* straw using NaOH, H_3PO_4, and $ZnCl_2$ for adsorptive removal of chromium from aqueous samples. Tadesse et al. [18] have reported *Teff* straw as a potential low-cost material for removing Cr (VI) from aqueous samples. Although these researchers have studied *Teff* straw as a potential low-cost material for biosorption of Cr (VI) from aqueous samples, they have not reported the response surface methodology parametric optimization (viz., concentration of acid/base, modification temperature, and time) of chemical modification of *Teff* straw using various acids and bases to enhance the adsorption capacity.

The present study has addressed (1) the synthesis of modified biosorbent using chemical modifying agents (H_3PO_4 and KOH) and characterization of the modified biosorbent from *Teff* straw biomass and (2) the effects of modification and optimization of process parameters (viz., concentration of the activating agent, activation temperature, and activation time) on the removal efficiency of Cr (VI) using the modified biosorbent from *Teff* straw. In addition, the kinetics and thermodynamics of Cr (VI) adsorption using modified biosorbent from *Teff* straw were also analyzed.

2. Materials and Methods

2.1. Materials. All chemicals used throughout this study were attaining the analytical reagent grade. The reagents were required to prepare stock solutions for chemical modification, adsorbate preparation, and dilution purposes. The Teff straw modification process required phosphoric acid, H_3PO_4 (purity 85.5%), and potassium hydroxide, KOH (98.08% pure). Sodium hydroxide, NaOH (98.08% pure), was employed for the determination of hemicellulose content of *Teff* straw, whereas sulfuric acid, H_2SO_4 (purity 98%), was used to determine the lignin content. Cr (VI) stock solution was prepared from potassium dichromate ($K_2Cr_2O_7$). All required solutions were prepared with analytical reagents using distilled water. 1,5-Diphenyl carbazide (DPC) was used to provide complexation with Cr (VI) and form pink color to determine the equilibrium concentration of residual Cr (VI) in the range of visible region in UV-visible spectrophotometer characterization. Methanol was required to dissolve the ligand DPC.

2.2. Equipment and Analytics. A laboratory test sieve (BS 410-1, Endecotts Ltd., England) was used to separate the required working size of the sample (pan to 0.50 mm). An electrical blender (OE-999, 220-240 V, 50/60 MHz, 350 W Seven 7 STAR, Germany) was employed to reduce the straw up to the desired average size. Digital balance (Mettler Toledo, 1118330367, 2000, Switzerland) was used to measure weights. Different size conical and Erlenmeyer flasks and beakers (Borosilicate Glass: 2000, 1000, 500, 250, 100, and 50 mL) were used in the preparation and dilution of the solutions.

A water bath (Weston-S-Mare Avon, Nickel Electro Ltd. 1008E, 50/60 Hz, 1000 W, England) was used to heat the solutions to determine the hemicellulose and lignin content of *Teff* straw. Jenway 3510 pH Meter (Barloworld Scientific Ltd., Dunmow, Essex, CM6 3LB, UK) was employed to fix the appropriate pH of the solution during the preparation of biosorbent and batch adsorption experiments. UV-visible spectrophotometer (Cary 50, Varian Australia Pty Ltd., Australia) was required to determine equilibrium concentrations of the adsorbate Cr (VI) after adsorption. Fourier transform infrared (FTIR) spectroscopy (IR Affinity-IS, Shimadzu, Japan) was used to determine the availability of organic and inorganic chemicals and/or functional groups that favor high adsorption capacity. Scanning electron microscope (SEM) (JEOL JCM-6000Plus, Germany) was provided to determine topography, morphological properties, essential information, crystallography, and orientation of grains, for acid- and base-treated straw. X-ray diffraction analysis (40 kV, 30 mA) was employed to analyze the crystalline structure of the prepared biosorbent on the adsorption capacity.

2.3. Collection and Pretreatment of Teff Straw. The natural *Teff* straw was collected from farmlands around *Bishoftu*, Ethiopia. The straw was thoroughly washed with tap water several times to eliminate the surface adhered particles and other soluble impurities. The washed samples were kept initially drying in sunlight for 12 h. After removing excess water content, the straw was transferred into an electric oven to eliminate extra moisture for 6 h at 105°C. In order to improve the modification process, the dried *Teff* straw was grounded and sieved to reduce cellulose crystallinity and attain homogenous particle-sized material in the range of pan to 0.50 mm using an electrical blender. The grounded straw was again washed thoroughly with hot distilled water to remove the extra impurities and soluble components like reducing sugars. Then, it was oven dried for 8 h, at 105°C. Finally, the untreated *Teff* straw (UTS) was placed in a well-dried and airtight desiccator for further use.

2.4. Biosorbent Preparation. The procedure followed by Doboy et al. [24] was adapted to prepare biosorbent from *Teff* straw biomass. The grounded and well-dried *Teff* straw was used to prepare a potential biosorbent by chemically modifying the original structure of the straw using H_3PO_4 and KOH as activating agents. Biosorbent preparations were carried out by applying batch reactor mode using separate identical beakers of 500 mL. During the preparation of biosorbent, the effects of process variables (viz, concentration of activating agents (H_3PO_4 and KOH), activation temperature, and activation time) were investigated in the case of one variable at a time (OVAT) by fixing other variables constant. The grounded dried material, i.e., UTS, was chemically modified on the heating mantel (450°C max.) with the help of a magnetic stirrer in the stated temperature scales. On the other hand, the concentration of activating agents and activation temperature vary (0.5, 1, 1.5, 2, 2.5, and 3 M and 40, 60, 80, 100, 120, and 160°C), respectively, for both activating agents. The activation temperature was adjusted by using a thermometer (250°C max.).

Moreover, the activation time was set at 1, 2, 3, 4, 5, and 6 h corresponding with activating agent concentration and activation temperature. Finally, 15 g of UTS sample was dehydrated with 100 mL of H_3PO_4 and KOH solutions of the activating agents. The reactor (beaker) was covered by aluminum foil throughout the modification process to prevent escaping of condensable materials. After the modification, the material was cooled at ambient temperature and washed with plenty of distilled water until the filtrate attains neutrality. Meanwhile, the modified and filtered *Teff* straw was transferred into an electric oven until attaining constant weight at 110°C. The resulting *Teff* straw biosorbent material is named as follows: acid-treated biosorbent (ATB) and base-treated biosorbent (BTB), modified with H_3PO_4 and KOH, respectively, as given in Figure 1.

2.5. Compositional Analysis of the Teff Straw. Agricultural wastes mostly contain three major compositional components, cellulose, lignin, and hemicellulose, along with trace amounts of pectin, protein, extractives, and ash [25, 26]. Determining structural components of lignocellulosic material is crucial to analyze the overall efficiency (i.e., the compositional analysis of biomass and its effects in the metal adsorption process) of the process designed to convert biomass to biosorbent. Mainly, the biosorption of metal ions depends on the available binding active sites of the biosorbent. However, the available binding active sites of the biosorbent are also dependent on the composition of the biomass, i.e., its cellulose, hemicellulose, and lignin. Thus, the modifying/activating agents such as acids and bases to enhance the available active sites of the original biomass altered these compositions of biomass [18, 25]. Various methods existed to examine the compositional constituents of given agricultural biomass, such as TGA, X-ray diffraction, and chemical analysis. However, the chemical gravimetric analysis is most promising than others due to its simplicity, economically viable, and readily available procedure to identify the constituents of the straw [24, 27, 28]. Specifically, under TGA, compositional analysis of biomass might have some errors. However, hemicellulose decomposed up to 270°C cellulose also decomposed 240–350°C, and lignin might be hydrolyzed 280–500°C [22, 24]. Therefore, the great challenge is that cellulose might be interfering in the structural value of others and vice versa at the specified temperature ranges. Thus, in this study, gravimetric analysis was employed to identify the amount of three lignocellulose components (cellulose, hemicellulose, and lignin) in straw by the method proposed by Abbas et al. and Maisyarah et al. ([27]; Maisyarah et al., 2019). Experiments under a compositional analysis of *Teff* straw were replicated three times and reported the average value of each result.

2.5.1. Determination of Extractives. The Soxhlet extraction unit setup was applied to separate extractive free biomass from extractive-laden material following the method represented by Adeeyo et al. [28]. 400 mL of acetone solvent was used to determine the extractive content with transferred 3.0 g dried straw (A) into cellulose thimble. The extraction process was carried out at 70°C for 4 h on the heating plate.

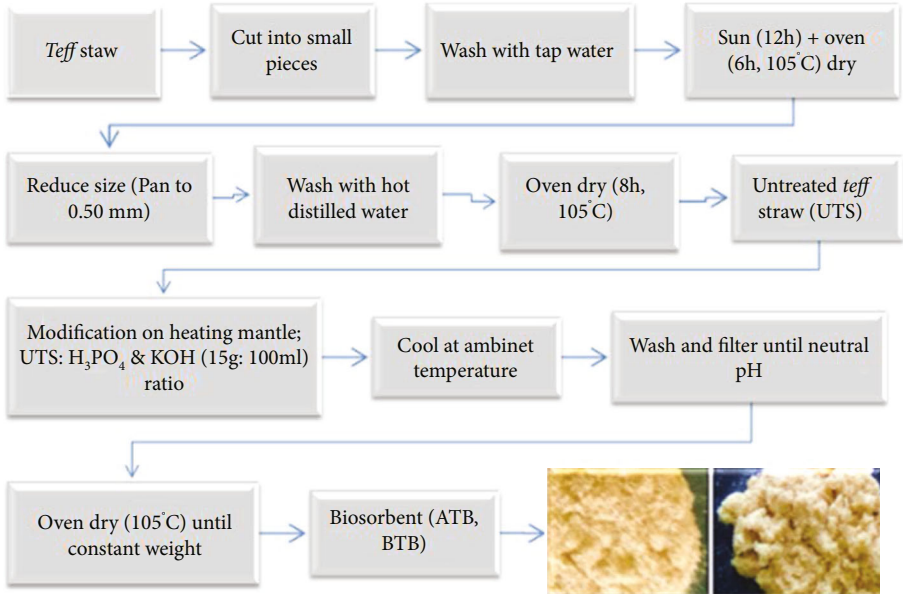

Figure 1: Schematic representation of *Teff* straw biosorbent preparation.

After 4 h extraction, the extracted material was dried in an electric oven at 110°C until a constant weight was obtained (B). Therefore, the amount of extractive (% *w*/*w*) was determined as

$$\frac{(A\text{-}B)}{A} * 100 = \text{Extractives(wt\%)}. \quad (1)$$

2.5.2. Determination of Hemicellulose Content. The hemicellulose content of *Teff* straw was determined using chemical gravimetric analysis [28] with some modification. 250 mL Erlenmeyer flask was required to mix 1 g of dried extractive-free UTS biomass (B) with 150 mL of 0.5 M sodium hydroxide (NaOH) and boiled at 80°C for 3.5 h in hot plate. The sample was washed with distilled water until neutral pH ≈7.0 and filtered through Whatman 42 filter paper. The sample was dried in an oven at 110°C until a constant weight (C). Finally, the hemicellulose content (% *w*/*w*) was determined by equation (2) subtracting the sample weight before and after hydrolysis of *Teff* straw by KOH solution.

$$\frac{(B - C)}{B} * 100 = \text{Hemicellulose(wt\%)}. \quad (2)$$

2.5.3. Determination of Lignin Content. The lignin content of *Teff* straw was also determined using chemical gravimetric analysis used by Adeeyo et al. [28] with some modification. First, 3 g of extractive-free sample (B) was transferred into 30 mL of 98% sulphuric acid in a 250 mL conical flask. At ambient temperature, the mixture was leftover 24 h. The black liquor was formed and then boiled at 120°C for 1 h on the hot plate. The soluble lignin derivates, lignosulfonates, formed by treating biomass at elevated temperatures (≈150°C) with solutions containing sulfate ions (1.5 to 3%). After filtering the mixture, the solid residue was washed using distilled water until the sulfate ion was undetectable. The washed water of sulfate ion was analyzed and/or detected via titration process with 10% of barium chloride solution obtaining precipitate in a colloidal form. The sample was dried in an oven at 110°C until a constant weight was obtained (D). The final insoluble lignin content (% weight) was determined.

$$\frac{(D - B)}{D} * 100 = \text{Lignin(wt\%)}. \quad (3)$$

2.5.4. Determination of Cellulose Weight. Considering an assumption that cellulose, hemicelluloses, lignin, and extractives are only components of the untreated *Teff* straw, the cellulose content was determined using the difference. Assuming 100% to the total amount of *Teff* straw sample applied in the experiment and then calculating the difference between the initial sample weight with other three components (viz., extractives, hemicellulose, and lignin) weight during the experimental process, the weight of cellulose (E) would be as represented in

$$(A - B) + (B - C) + D = \text{Weight of Cellulose}(E). \quad (4)$$

2.6. Batch Biosorption Studies. An adsorption equilibrium data is critical to provide optimum parameters and understand the mechanism of adsorption. This study used batch adsorption experiments to investigate parametric effects such as contact time, biosorbent dosage, initial Cr (VI) concentration, and temperature. The 1000 mg/L Cr (VI) synthetic stock solution was prepared by adding 0.1 g of dried $K_2Cr_2O_7$ in 100 mL distilled water in a volumetric flask. To examine effect of parameters, contact time (1-6 h), initial Cr (VI) concentration (50-200 mg/L), biosorbent dosage

(0.5, 1, 1.5, 2, 2.5, and 3 g), and temperature (25-50°C) were applied. The Cr (VI) solutions were taken in a 250 mL conical flask with the pH adjustment at 2. The solutions were stirred at a constant speed in an automatic shaker to achieve a high interfacial contact area for a better mass transfer process. Vacuum filtration was applied to separate the supernatant from the chromium-containing biosorbent. Finally, the remaining or residual concentrations of Cr (VI) were determined by a Varian UV-visible spectrophotometer ($\lambda_{max} = 542$ nm). The removal efficiency, $R(\%)$, and adsorption capacity, q_e, of Cr (VI) metal ion onto the treated *Teff* straw biosorbent were determined using the mass balance equations (5a) and (5b), respectively. The adsorption isotherm, kinetic, and thermodynamic experiments were fundamental in describing the characteristics of biosorbent and designing any adsorption system.

$$R(\%) = \left(\frac{C_o - C_e}{C_o}\right) * 100, \tag{5a}$$

$$q_e = \left(\frac{C_o - C_e}{m}\right) * V. \tag{5b}$$

2.7. Adsorption Isotherm Studies. Langmuir and Freundlich's models were the most widespread and preferred expression of adsorption equilibrium applied in vast adsorbate concentrations. Shokoohi et al. [29] adopted the assumptions in the Langmuir model: monolayer coverage, all surface sites are alike and only can accommodate one adsorbed atom, and the ability of a molecule to be adsorbed on a given site independent of its neighboring sites occupancy. Based on these assumptions and a kinetic principle (rate of adsorption and desorption from the surface is equal), the Langmuir equation can be written in the general form of nonlinear equation (6a). The values of q_{max} and K_L were evaluated from the slope and the intercept of the linear forms of Langmuir isotherm.

$$q_e = q_{max} \frac{K_L C_e}{1 + K_L C_e}, \tag{6a}$$

$$\frac{C_e}{q_e} = \frac{1}{q_{max}} C_e + \frac{1}{K_L q_{max}}, \tag{6b}$$

$$\frac{1}{q_e} = \left(\frac{1}{K_L q_{max}}\right) \frac{1}{C_e} + \frac{1}{q_{max}}, \tag{6c}$$

$$\frac{q_e}{C_e} = K_L q_{max} - K_L q_e, \tag{6d}$$

where q_e is the amount of adsorbate adsorbed on the biosorbent in the equilibrium (mg/g), q_{max} is the maximum adsorption capacity corresponding to a complete monolayer coverage (mg/g) on the adsorbent surface, C_o and C_e are initial and equilibrium concentrations of metal ion Cr (VI) (mg/L), K_L is the Langmuir constant (L/mg), V is the volume of the Cr (VI) solution (L), and m is the weight of the biosorbent that participates in the adsorption process (g). The characteristic of the Langmuir isotherm can be expressed in terms of a dimensionless factor, R_L, as shown in

$$R_L = \frac{1}{(1 + b_L * C_o)}. \tag{7}$$

The R_L values were indicated the type of adsorption as either unfavorable ($R_L > 1$), linear ($R_L = 1$), favorable ($0 < R_L < 1$), or irreversible ($R_L = 0$). At the same time, the Freundlich isotherm can be applied for nonideal adsorption on heterogeneous surfaces and multilayer adsorption. Moreover, the Freundlich model is an empirical and semiempirical model that describes heterogeneous systems nonlinearly (equation (8a)) and linearized logarithm form (equation (8b)). The plot of log q_e versus log C_e has been contributed a slope value of $1/n$ with an intercept magnitude of log K_F. On average, favorable adsorption tends to have the Freundlich constant n between 1 and 10. A smaller value of $1/n$ implies more vital interaction between biosorbent and heavy metal, and $1/n$ equal to 1 indicates linear adsorption leading to identical adsorption energies for all sites.

$$q_e = K_F C_e^{1/n}, \tag{8a}$$

$$\log q_e = \log K_F + \frac{1}{n} \log C_e. \tag{8b}$$

2.8. Adsorption Kinetic Studies. Adsorption kinetic studies were conducted in batch reactions using 100 mL of Cr (VI) solution with 100 mg/L initial concentration of Cr (VI) in 250 mL Erlenmeyer flasks at constant pH (=2). 1 g of treated *Teff* straw biosorbent was added to the solution and agitated in the shaker at 30, 40, 50, and 60°C and analyzed at a time interval of 1 to 6 h. The adsorption kinetics was analyzed by pseudo-first-order and pseudo-second-order models. According to the procedure described by Overah [30], the linear functions of pseudo-first- and pseudo-second-order kinetic models are given in equations (9a) and (9b), respectively.

$$\log (q_e - q_t) = \log q_e - \frac{K_1 t}{2.303}, \tag{9a}$$

$$\frac{t}{q_t} = \frac{1}{K_2 q_e^2} + \frac{t}{q_e}, \tag{9b}$$

where q_e and q_t are the amount of Cr (VI) adsorbed on the adsorbent at equilibrium and at any time, respectively (mg/g), K_1 is the pseudo-first-order rate constant (min^{-1}), and K_2 ($g\,mg^{-1}\,min^{-1}$) is the pseudo-second-order rate constant. Therefore, K_1 and K_2 can be calculated from the slope and intercept of the plot of log $(q_e - q_t)$ versus t and t/q_t against t, respectively.

2.9. Thermodynamic Studies. Thermodynamic studies under the biosorption process showed us the spontaneity of the process, i.e., whether the process is spontaneous or not. The main parameters analyzed under thermodynamic

studies were Gibb's free energy (ΔG^o), enthalpy (ΔH^o), and entropy (ΔS^o) which can be determined by

$$\Delta G^o = -RT \ln K_L,$$
$$\ln K_L = \frac{\Delta S}{R} - \frac{\Delta H}{RT}, \quad (10a)$$

where R is the gas constant (8.314 J/mol K), K_L is the Langmuir isotherm constant at different temperatures (L/mg), and T is the absolute temperature in Kelvin.

3. Results and Discussion

3.1. Effect of Modification Parameters on the Adsorption Capacity of Biosorbent. As mentioned in Introduction, the modification variables (viz., agent concentration, activation temperature, and activation time) significantly affect the adsorption capacity of *Teff* straw biosorbent. Modification of the *Teff* straw plays a significant role in increasing porosity and specific surface area of the biosorbent. In this study, the chemical activation method was employed using base (KOH) and acid (H_3PO_4) activating agents that significantly affect the extent of activation. Strong base activation resulted in highly microporous adsorbents with high surface areas and created more active reaction sites than other activating agents [23, 31–33]. In this study, maximum adsorption capacity attained with acid- and base-treated *Teff* straw were 9.2 and 9.5 mg/g, respectively. KOH modification of *Teff* straw has increased the concentration of oxygen molecules of hydroxide, which strongly reacts with metal ions, whereas in H_3PO_4 treated, bulk phosphate groups cannot pass fast in the aqueous solutions resulting in adsorption capacity of Cr (VI) onto *Teff* straw surface to decrease. Generally, the results show that *Teff* straw was a potential biosorbent prepared at 1.75 M, 100°C, and 3.5 h for both activating agents (KOH and H_3PO_4). All three process variables (viz., activating agent concentration, activation temperature, and activation time) were investigated with the corresponding value of percentage yield and removal efficiency of Cr (VI). The percentage yield was determined from equation (11), and the removal efficiency, $R(\%)$, of Cr (VI) metal ion has been determined as mentioned in the previous section in equation (5a).

$$\text{Yield}(\%) = \frac{W_c}{W_o} * 100. \quad (11)$$

3.1.1. Effect of Activation Temperature. The activation temperature ranges from 40 to 160°C were performed for both activating agents (H_3PO_4 and KOH) by fixing the concentration of chemical activating agents and activation time at 1 M and 3 h, respectively. The percent yield (yield%) and removal efficiency of the activated biosorbent changed significantly with activating agents. The activation with H_3PO_4 and KOH resulted in the highest percentage yield of 91.67 and 88.60%, respectively. This result indicated that KOH solubilizes the lignin structure of biomass, while H_3PO_4 also decomposed only the cellulose and hemicellulose structure of the straw. The activation temperature increased causing a decrease in the yield values due to more volatile matter from the straw. Therefore, the final biosorbent dry weight becomes lesser than the precursor dry weight of the base-treated *Teff* straw. Figure 2(a) shows that the yield (%) decreased whereas removal percentage, $R(\%)$, increased with increasing activation temperature due to the release of functional groups with acid and base treatment. Beyond 120°C removal efficiency, $R(\%)$ slightly decreased due to reduction of average pore diameter because of narrowing of the pores, resulting in contraction of the newly formed pores [34, 35]. The activation process, relatively at a low operating temperature, significantly reduced the energy consumption and operating cost.

3.1.2. Effect of the Activation/Modification Time. During the activation process, the activation agent concentration and temperature were kept constant at 80°C and 1 M, respectively. The effect of activation time on the yield (%) and $R(\%)$ of the biosorbent product is shown in Figure 2(b). It has been observed that the value of removal efficiency steeply increased with time of activation and leveled off after 4 h. Thus, the prolonged activation time would promote the diffusion of activating agents in the *Teff* straw; this idea agreed with Msagati et al. and Lou [35, 36]. However, beyond 4 h, no significant change in $R(\%)$ was found. Meanwhile, the yield (%) decreases with increasing activation time in both chemical agents.

3.1.3. Effect of Activating Agent Concentration. The activating agents' concentrations were set at 0.5, 1.5, 2, 2.5, and 3 M to investigate the effect of different concentrations on the yield (%) and $R(\%)$. In Figure 2(c), the yield (%) and $R(\%)$ decreased and increased with increasing chemical active agent concentration from 0.5 to 3 M in both chemical agents, respectively. Li et al. [37] have examined that the activation efficiency was strengthened with the increment of the activating agent concentration. Nevertheless, in the present work, $R(\%)$ using an activating agent at levels higher than 3 M did not increase but slightly decreased activation efficiency. This result is because the excessive amount of activating agent concentration might have accumulated on the surface of the *Teff* straw.

3.2. Characterization of Teff Straw and Modified Biosorbent. Both untreated and modified *Teff* straw were subjected to the physicochemical characterization that determines the adsorption capacity of the biosorbent, i.e., the compositional analysis of *Teff* straw, Fourier transform infrared (FTIR) spectroscopy, scanning electron microscope (SEM), X-ray diffractometer (XRD), and UV-visible spectrophotometer analysis.

3.2.1. Compositional Analysis of Teff Straw. Cellulose, hemicellulose, and lignin content of *Teff* straw were determined using chemical gravimetric analysis as cellulose = 41.68 wt%, hemicellulose = 38 wt%, and lignin = 17.00 wt% on a dry basis. The extractive content was determined using the Soxhlet apparatus as 3.32 wt% on a dry basis. The results of the present study are comparable with the previous

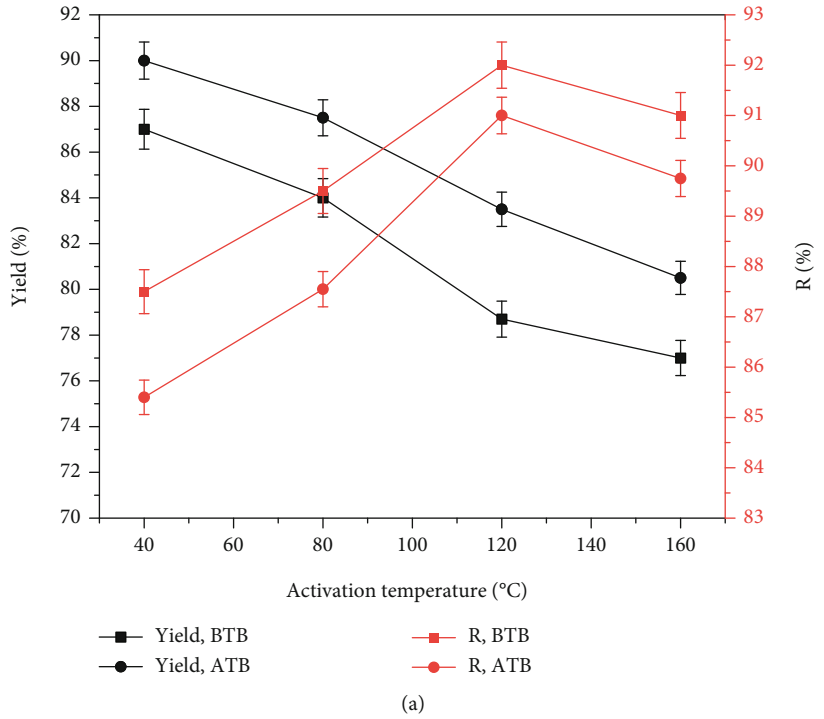

(a)

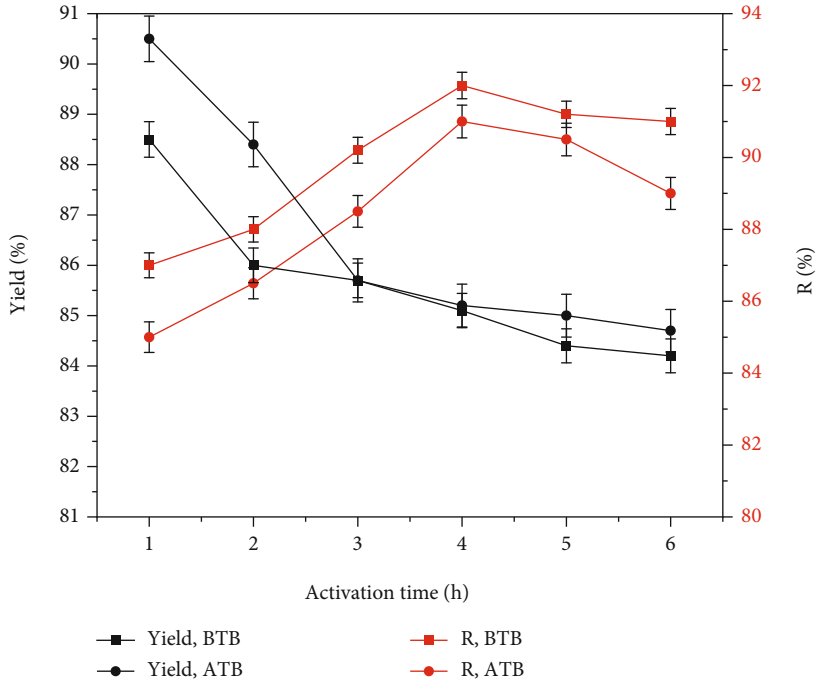

(b)

Figure 2: Continued.

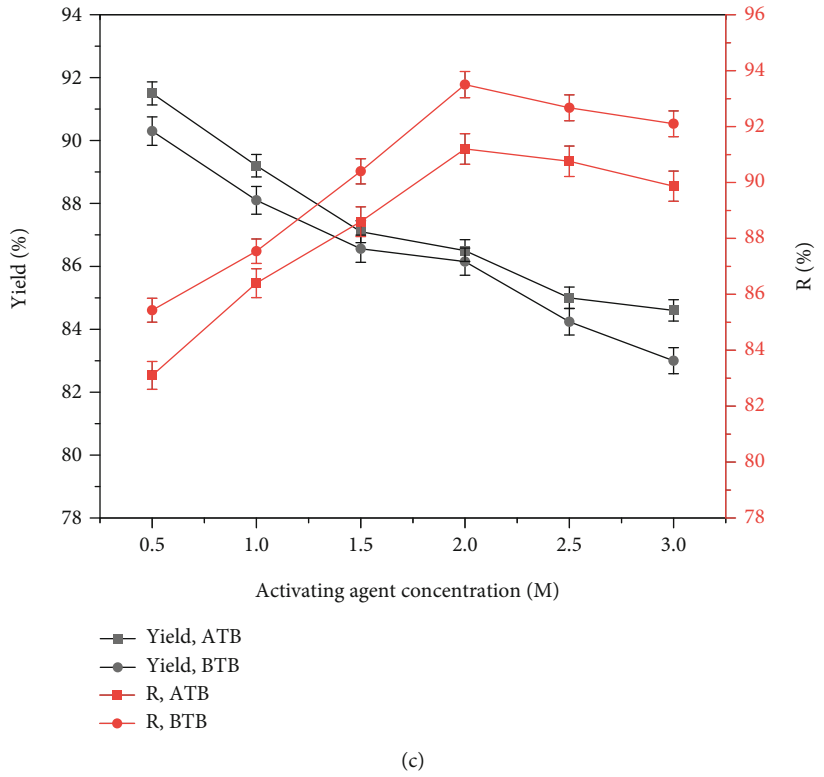

(c)

Figure 2: Results of yield (%) and R(%) of biosorbent on (a) modification temperature, (b) modification time, and (c) activating agent concentration.

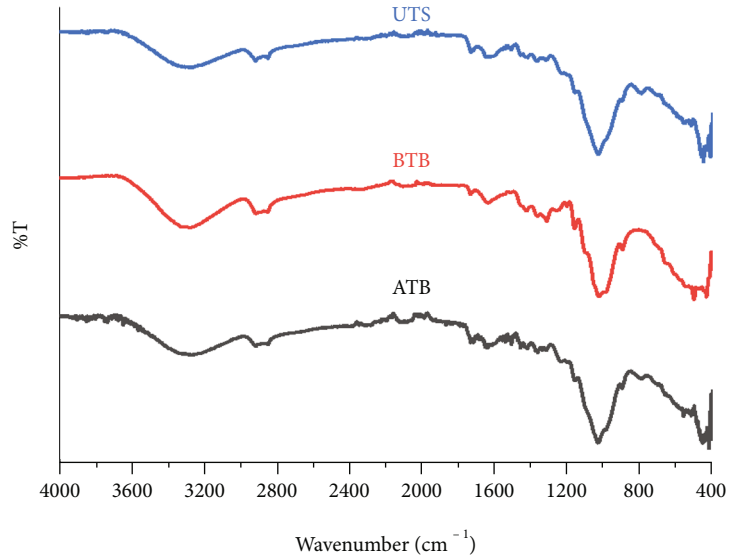

Figure 3: FTIR spectral of the raw and treated *Teff* straw.

literature with some deviation in the source of biomass (whether woody, nonwoody, etc.), geographical locations of materials, methods of analysis, the difference in solvents, and biomass variety (Ayeni et al., 2015; [26]).

3.2.2. Fourier Transform Infrared (FTIR) Spectroscopy Analysis. The FTIR spectra of raw and chemically modified natural *Teff* straw biosorbent were used to determine the functional groups' availability and vibrational frequency changes capable of binding metal ions. Different biomass has various types and amounts of binding groups that actively participate in adsorption. Figure 3 shows that *Teff* straw has some functional groups such as hydroxyl (-OH), amino (NH_3^+), carboxyl (-CH_2COOH), C=O), and amide

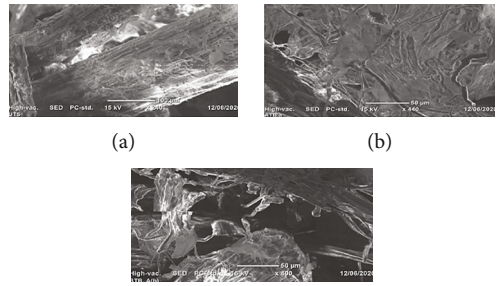

(a) (b)

(c)

Figure 4: The SEM micrographs of (a) UTS, (b) ATB, and (c) BTB.

(-$CONH_2$) that are involved in the removal of Cr (VI) metal ions. The peak in the range of 1700-1450 cm^{-1} due to carboxylic and carbonyl groups from aldehydes, ketones, and aromatic rings from the lignin part is not detected after KOH treatment of *Teff* straw due to lignin removal. In the peak range of 1700-1450 cm^{-1}, stretching vibration caused by -C=O vanished for the KOH treatment *Teff* straw as compared with the untreated Teff straw, which inferred that the addition reaction might be happened in the -C=O group. Moreover, the band at 1251.00 cm^{-1} triggered by -C-O- group divided into two small peaks, which showed that some substitution reaction took place on the side chain of -C-O- group. Thus, the results of FTIR showed that the improved adsorption efficiency of *Teff* straw due to KOH modification resulted from the increase of ether bond [23, 32, 33]. From 3700-3150 cm^{-1}, peak range of -OH group stretching vibration, in both untreated and chemically modified *Teff* straw, is observed due to the presence of water. Therefore, it is predictable that peak strength rises in some functional groups owing to the increment in surface area and loss of specific functional group as a result of removal of specific lignocellulosic portion during chemical activation.

3.2.3. Scanning Electron Microscope (SEM) Analysis. SEM analysis has been employed to observe the surface texture and morphology changes of both untreated and chemically modified biosorbents. The SEM images of untreated and chemically modified *Teff* straw biosorbents are given in Figure 4. The untreated *Teff* straw biosorbent, UTS, shows a relatively smooth surface (Figure 4(a)). However, after H_3PO4 and KOH modification, the presence of pores and cracks made the surface of *Teff* straw more uneven and irregular (Figures 4(b) and 4(c)), which may be more helpful for adsorption. Specifically, for KOH-modified biosorbent, BTB shows significant surface modification (Figure 4(c)) that developed honeycomb, rough surfaces, nonuniform pores, and cavities. These were due to lignin and hemicellulose structure removal during the reaction between KOH and ester bonds. Nevertheless, H_3PO_4-modified *Teff* straw showed somehow lesser porous surface structures (Figure 4(b)) than KOH-modified *Teff* straw due to less reactivity of the phosphate groups.

3.2.4. X-Ray Diffractometer (XRD) Analysis. Figures 5(a)–5(c) depict XRD patterns of the untreated (UTS) and chemically modified *Teff* straw with acid (ATB) and base (BTB), respectively. In order to observe the crystalline structure of *Teff* straw biomass, X-ray diffractometer equipped with copper (Cu) radiant source with energy of 40 kV, an electric current of 30 mA, scanning speed of 3°/min, and scanning range of 10 to 80 degrees was carried out.

As shown in Figure 5(c), peak height formed due to the diffraction of crystalline regions of cellulose around 2θ of 22° increased in KOH-treated Teff straw compared to the untreated and acid-treated *Teff* straw. From XRD data, the area of all crystalline peaks (10876.42, 12081.26, and 10959.6) and area of all peaks (18048.3, 18838.56, and 16159.36) of untreated and modified *Teff* straw, respectively, could be found using Origin-pro and Excel software. The crystallinity index (equation (12a)) of UTS was found to be 60.3%. The crystallinity index increased from 60.3% to 64.1% and 67.8% with ATB- and BTB-modified *Teff* straw. The increase in the crystallinity of KOH-modified *Teff* straw is due to removing hemicellulose and lignin content. In XRD data, the broadening (β_T) of peaks is due to the combined effect of crystallites size (β_D) and microstrain ($\beta\varepsilon$) that can be expressed as equation (12b). From the D. Scherer equation, the crystallite size was determined in equation (12c). Similarly, the XRD peak broadening due to microstrain has been given by equation (12d). This equation represents a straight line, ε is the ratio between two lengths (slope) of the line (dimensionless quantity), and $K\lambda/D$ is the y-intercept by determining FWHM and peak position from XRD data. W-H plot y-intercept ($K\lambda/D$) is 0.19383, and slope (ε) is 0.02615. Therefore, the crystallite size of ATB is 0.75 nm. Similarly, UTS and BTB are 4.9×10^{-3} and 0.113 nm, respectively.

$$\text{Crystallinity} = \frac{\text{Area of crystalline peaks}}{\text{Area of all peaks}} * 100, \quad (12a)$$

$$\beta_T = \beta_D + \beta_\varepsilon, \quad (12b)$$

$$\text{D} = \frac{K\lambda}{\beta_D \cos\theta}, \quad (12c)$$

$$\beta_\varepsilon = 4\varepsilon \tan\theta, \quad (12d)$$

where β_T is the total broadening, β_D is the broadening due to the crystallite size, β_ε is the broadening due to strain, β_D is

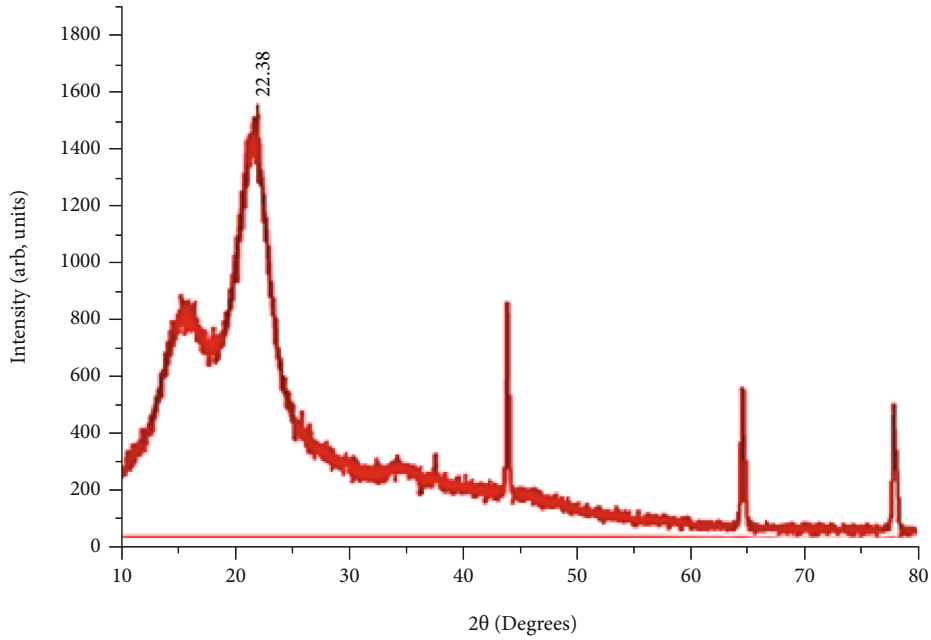

(a)

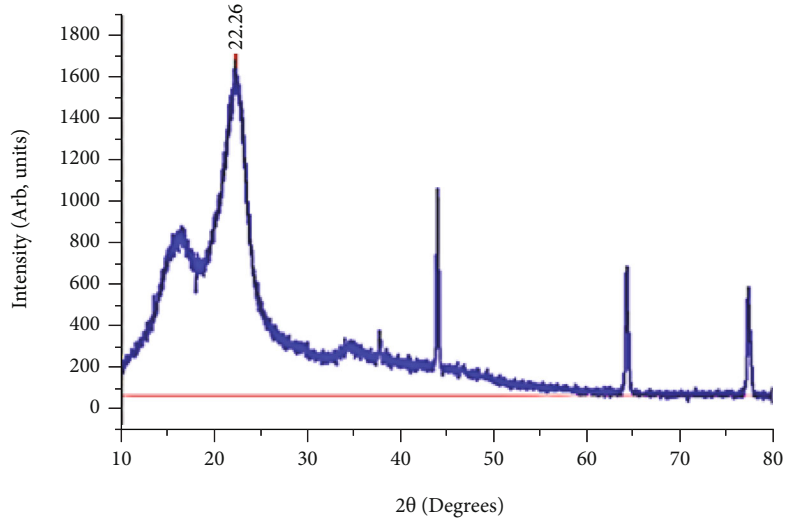

(b)

Figure 5: Continued.

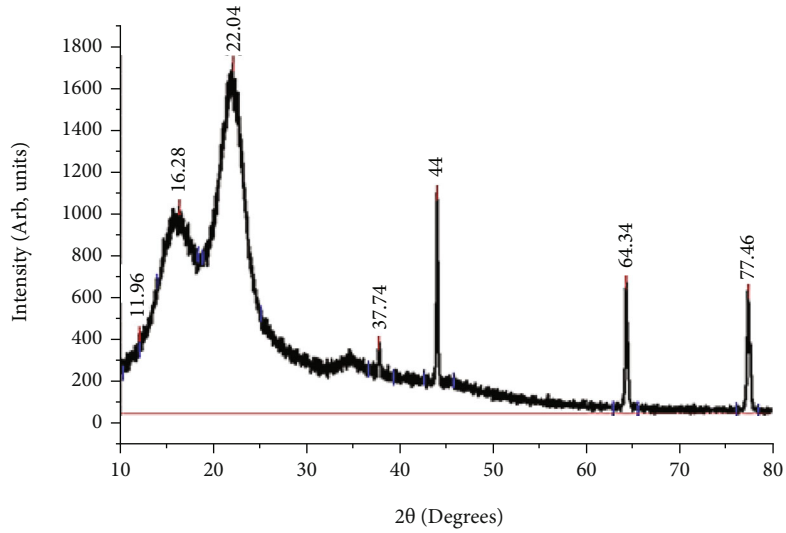

(c)

Figure 5: XRD patterns of untreated and treated *Teff* straw: (a) UTS, (b) ATB, and (c) BTB.

Table 1: Independent variables' range and level: (a) the BBD of the experimental matrix with experimental and predicted values for ATB and BTB (b).

(a)

Variable	Symbol	Unit	Range and level		
			-1	0	+1
Activating agent concentration (H_3PO_4, KOH)	A	M	0.5	1.75	3
Activation temperature	B	˚C	40	100	160
Activation time	C	Hr	1	3.5	6

(b)

Std order	H_3PO_4 conc. (M)	Activation temp. (˚C)	Activation time (hr)	Cr (VI) removal (%)			
				Exp (1)	Pred (1)	Exp (2)	Pred (2)
1	0.5	40	3.5	84.67 + 0.017	85.38	86.54 + 0.024	86.53
2	1.75	40	6	87.30 + 0.025	86.96	88.15 + 0.019	88.15
3	3	160	3.5	91.25 + 0.036	90.54	87.65 + 0.041	87.66
4	1.75	100	3.5	92.30 + 0.039	92.30	95.20 + 0.028	95.20
5	1.75	160	1	87.10 + 0.021	87.44	87.74 + 0.013	87.74
6	0.5	100	1	86.23 + 0.010	86.15	86.82 + 0.027	86.87
7	0.5	100	6	88.62 + 0.061	88.26	89.23 + 0.057	89.24
8	3	100	1	87.20 + 0.053	87.57	88.50 + 0.063	88.49
9	1.75	40	1	84.50 + 0.047	83.87	87.24 + 0.041	87.20
10	1.75	100	3.5	92.30 + 0.043	92.30	95.20 + 0.048	95.30
11	3	40	3.5	86.50 + 0.062	86.76	88.00 + 0.054	88.05
12	3	100	6	90.75 + 0.016	90.83	88.45 + 0.031	88.40
13	0.5	160	3.5	88.20 + 0.042	87.94	88.43 + 0.038	88.38
14	1.75	160	6	89.10 + 0.059	89.73	89.03 + 0.051	89.07
15	1.75	100	3.5	92.30 + 0.046	92.30	95.20 + 0.026	95.20

1: acid-modified biosorbent (ATB); 2: base-modified biosorbent (BTB); Exp: experimental; Pred: predicted.

Table 2: ANOVA for the surface response model of Cr (VI) removal efficiency: (a) ATB and (b) BTB.

(a)

Source	Sum of squares	Df	Mean square	F-value	P value Prob > F	Comment
Model	146.10	9	16.23	1653.08	<0.0001	Significant
A	6.84	1	6.84	697.05	<0.0001	
B	20.54	1	20.54	2092.06	<0.0001	
C	21.52	1	21.52	2191.12	<0.0001	
AB	0.60	1	0.60	61.16	0.0005	
AC	10.73	1	10.73	1092.22	<0.0001	
BC	0.82	1	0.82	83.40	0.0003	
A^2	32.05	1	32.05	3263.82	<0.0001	
B^2	32.49	1	32.49	3308.28	<0.0001	
C^2	33.59	1	33.59	3420.75	<0.0001	
Residual	0.049	5	9.820E-003			
Lack of fit	0.049	3	0.016			
Pure error	0.000	2	0.000			
Cor total	146.15	14				

(b)

Source	Sum of squares	Df	Mean square	F-value	P value Prob > F	Comment
Model	132.56	9	14.73	5915.19	<0.0001	Significant
A	0.31	1	0.31	125.32	<0.0001	
B	1.07	1	1.07	428.03	<0.0001	
C	2.60	1	2.60	1043.86	<0.0001	
AB	1.25	1	1.25	503.78	<0.0001	
AC	1.51	1	1.51	607.59	<0.0001	
BC	0.036	1	0.036	14.50	0.0125	
A^2	49.66	1	49.66	19945.22	<0.0001	
B^2	55.51	1	55.51	22294.73	<0.0001	
C^2	39.78	1	39.78	15977.47	<0.0001	
Residual	0.012	5	2.490E-003			
Lack of fit	0.012	3	4.150E-003			
Pure error	0.000	2	0.000			
Cor total	132.57	14				

the FWHM (broadening of the peak) in radians, K is the shape factor, 0.94 (constant), λ is the wavelength of X-ray source (0.15406 nm), θ is the position of the peak in radians, β_ε is broadening due to strain, and ε is strain.

The XRD analysis results showed that both crystallinity index and crystallite size increased with acid- and base-treated *Teff* straw biosorbent due to removing amorphous lignin and hemicellulose with cellulose domination [23, 32, 33].

3.3. Optimization of Process Variables for Teff Straw Modification. Box-Behnken design (BBD) under response surface methodology (RSM) was conducted to study the effects of independent process parameters (viz., activating agent concentration, modification time, and temperature) involved in the preparation of *Teff* straw-based biosorbent and their interaction that affects the characteristic of biosorbent and biosorption efficiency to remove Cr (VI) metal ions. The response was optimized using Design Expert 7.0 statistical software tools through a two-level three-factor design via RSM to develop correlations between the biosorbent preparation variables and the response value that is Cr (VI) $R(\%)$. It required 15 runs with 3 independent factors for a 3-level design with three center points. For each experimental run, Cr (VI) removal efficiency was determined using the methodology described. The independent variables' range and level are indicated in Table 1 (a). Based on the sequential model sum of squares, highest order polynomials where the additional terms were significant and models were not aliased were used to select the models.

3.3.1. Optimization of Process Variables for Biosorption of Cr (VI) Using ATB. The positive coefficient values in equations

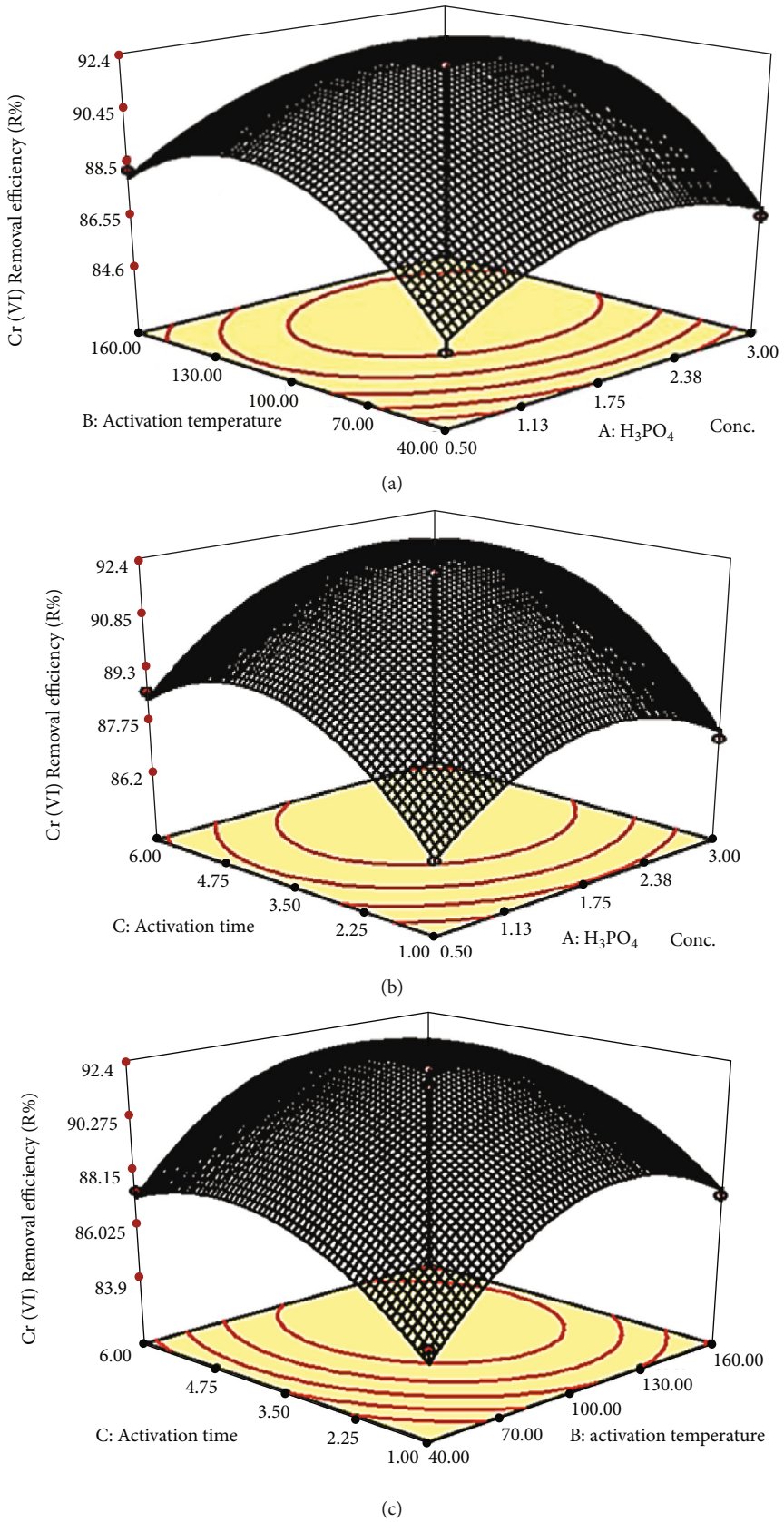

Figure 6: Surface plots of acid-treated *Teff* straw biosorbent Cr (VI) removal efficiency. (a) H_3PO_4 concentration vs. activation temperature, (b) H_3PO_4 concentration vs. activation time, and (c) activation temperature vs. activation time.

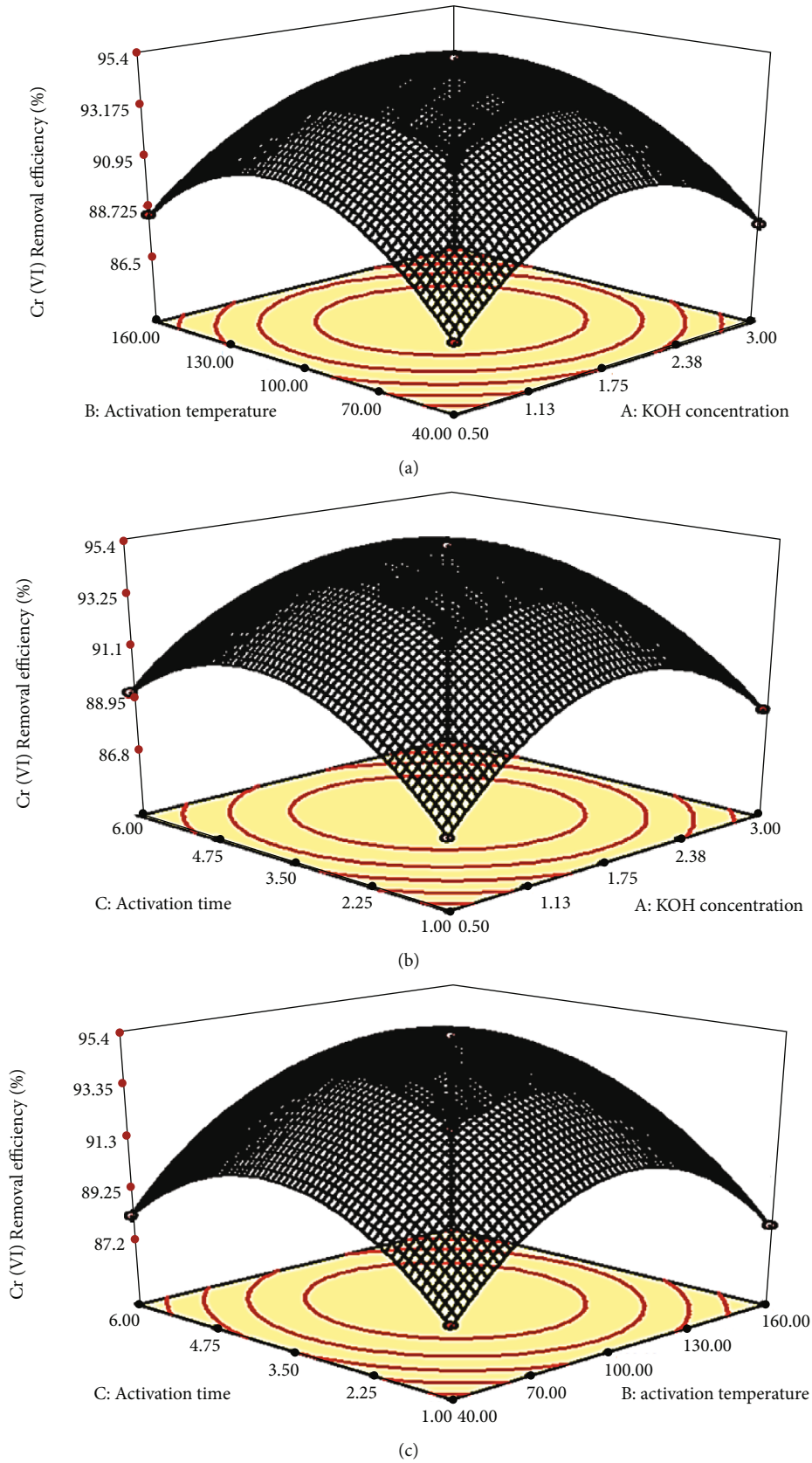

Figure 7: Surface plots of base-treated *Teff* straw biosorbent for Cr (VI) removal efficiency: (a) KOH concentration vs. activation temperature, (b) KOH concentration vs. activation time, and (c) activation temperature vs. activation time.

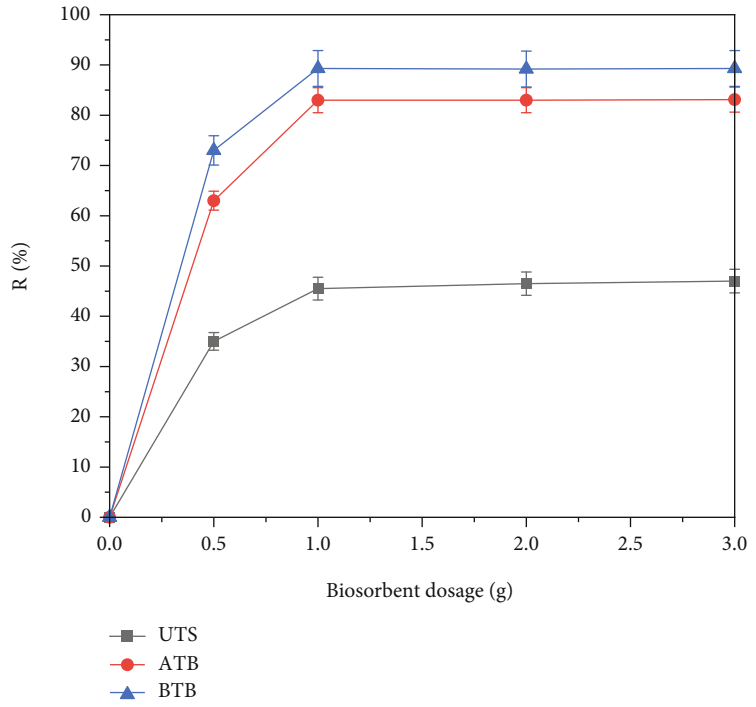

(a)

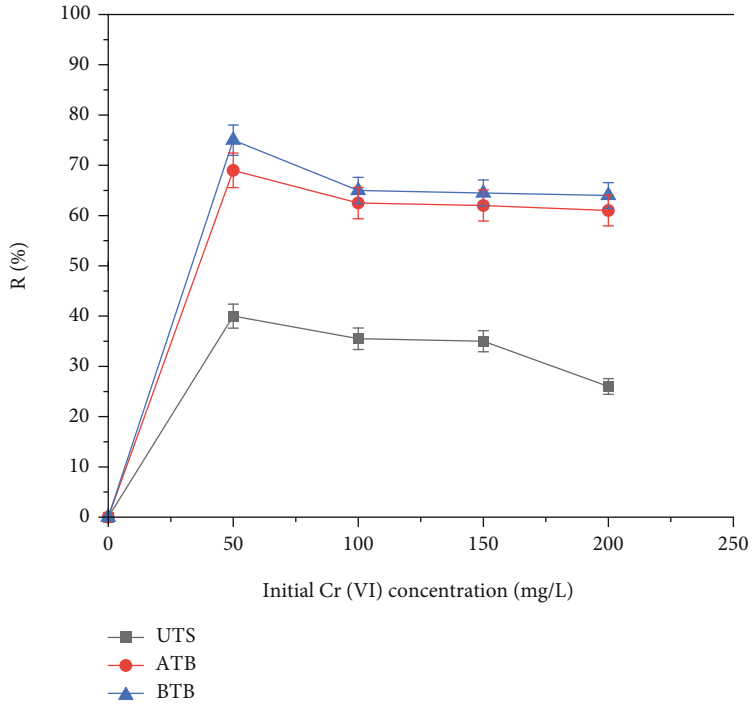

(b)

Figure 8: Continued.

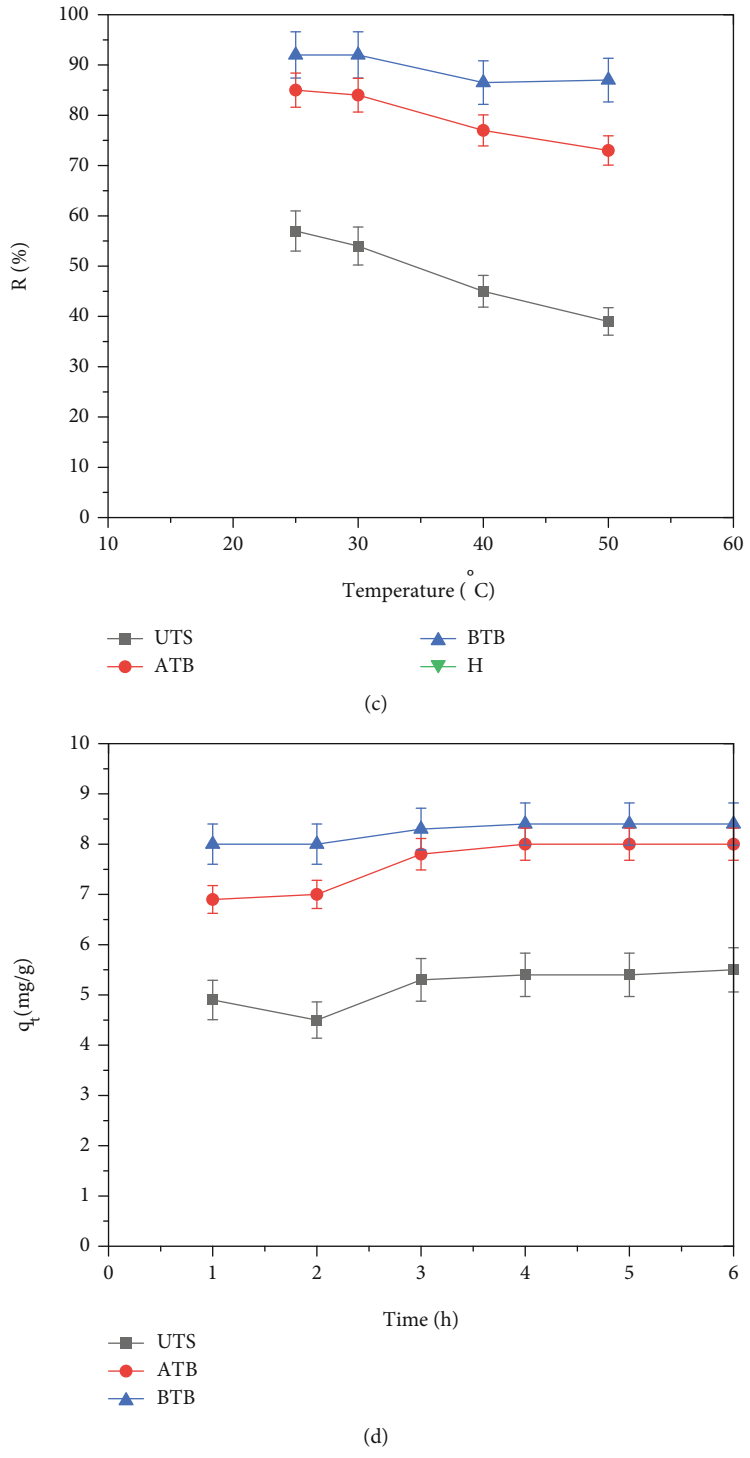

Figure 8: Effect of parameters on adsorption capacity of Cr (VI) metal ion: (a) biosorbent dosage, (b) initial Cr (VI) metal ion concentration, (c) temperature, and (d) contact time.

(13a) and (13b) indicated the positive interaction and impact of factors on the biosorption process, whereas the detrimental and interfering effect of the parameters on overall adsorption capacity is from negative coefficient value points. In order to identify the relevant model terms and fit the generated experimental data, the highest order polynomial empirical equation for Cr (VI) removal efficiencies (Y_A) could be represented as equation (13a) in terms of coded factors. The BBD of the experimental matrix with experimental and predicted values for acid- and base-modified *Teff* straw biosorbents is shown in Table 1 (b). The "Pred R-Squared" of 0.9946 is in reasonable agreement with the "Adj R-Squared" of 0.9991, which means the difference between "Adj R-Squared" and "Pred R-Squared"

Table 3: Isotherm and kinetic constants for Cr (VI) adsorption onto unmodified and modified *Teff* straw biosorbent.

(a)

Biosorbent	Langmuir isotherm parameters				Freundlich isotherm parameters		
	q_m (mg/g)	K_L (L/mg)	R^2	R_L	K_F (mg/g)	$1/n$	R^2
UTS	16.90	1.11	0.9956	0.0090	$8.90 * 10^{-23}$	0.066	0.9879
ATB	23.04	0.512	0.9975	0.020	$6.52 * 10^{-6}$	0.205	0.9734
BTB	23.585	0.281	0.9966	0.034	$7.65 * 10^{-4}$	0.300	0.9887

(b)

Biosorbent	Pseudo-first-order kinetics			Pseudo-second-order kinetics		
	q_e (mg/g)	k_1 (hr^{-1})	R^2	q_e (mg/g)	k_2 (g/mg hr)	R^2
UTS	0.970	-0.435	0.8322	3.32	0.31	0.8316
ATB	1.630	-0.591	0.8296	9.40	0.264	0.9959
BTB	1.90	-0.949	0.8568	9.60	0.394	0.9978

should be less than 2 with the value of 0.0045. "Adeq Precision" measures the signal-to-noise ratio. A ratio of 125.631, which is greater than 4, is desirable for the Cr (VI) removal efficiency model indicating the adequacy of signal and, in turn, stresses that the model can be used to navigate the design space. The ANOVA output (Table 2 (a)) shows that the model F-value of 1653.08 implies a significant model. There is only a 0.01% chance that a "model F-value" this large could occur due to noise. The values of $P > F$ less than 0.0500 indicate that model terms are significant. In this case, the models A, B, C, AB, AC, BC, A^2, B^2, and C^2 are significant model terms. Values greater than 0.1000 indicate that the model terms are not significant.

Figure 6 shows 3D response surface plots for the interaction effects of the independent variables on the Cr (VI) removal efficiency of the acid-treated biosorbent. Figure 6(a) depicts the combined effect of activating agent concentration versus activation temperature on the removal efficiency of Cr (VI) by fixing the activation time at the center point (3.5 h). The increase inactivating agent concentration and activation temperature improved the Cr (VI) removal efficiency slightly at the beginning. This effect was due to the formation of uniform porous structure and evolution of condensable and noncondensable volatile substances. In contrast, higher temperature and concentration of activating agent causes the widening of micropores to mesopores and macropores, thereby decreasing the performance of adsorbents [38]. The optimum values for maximum Cr (VI) removal efficiency of 92.5% under this model was as follows: 2 M, 110°C, and 4 h of concentration of the activating agent, activation temperature, and activation time, respectively, by using acid-treated *Teff* straw biosorbent.

3.3.2. Optimization of Process Variables for Biosorption of Cr (VI) Using BTB. Figure 7 shows 3D response surface plots for the interaction effects of the independent variables on the Cr (VI) removal efficiency of the acid-treated biosorbent. Table 2 (b) shows the ANOVA results for the response surface quadratic model. Large F-values of the model, linear quadratic, and interaction variables indicate the significance of the individual effect of the independent variables and the magnitude of interactions between them. Small P values confirm this result (P value ≤ 0.05) as shown in Table 2 (a and b).

Significant model terms are A, B, C, AB, AC, BC, A^2, B^2, and C^2. Model terms with values greater than 0.1000 are not significant. Model reduction may improve the model if there are many nominal terms (not counting those required to support hierarchy). The "Pred R-Squared" of 0.9985 is in reasonable agreement with the "Adj R-Squared" of 0.9997. "Adeq-Precision" measures the signal-to-noise ratio. A ratio greater than 4 is desirable. The ratio of 212.735 indicates an adequate signal. In order to fit the generated experimental data and to identify the relevant model terms, the most widely used highest order polynomial empirical equation for Cr (VI) removal efficiencies (Y_B) can be represented as the equation (13b) in terms of coded factors. The optimum values for maximum Cr (VI) removal efficiency of 95.2% under this model were as follows: 1.5 M, 105°C, and 3.5 h of concentration of the activating agent, activation temperature, and activation time, respectively, by using base-treated *Teff* straw biosorbent.

$$Y_A = [+92.30 + 0.92A + 1.60B + 1.64C - 0.39AB - 1.64AC - 0.45BC - 2.95A^2 - 2.97B^2 - 3.02C^2], \quad (13a)$$

$$Y_B = [+95.20 + 0.20A + 0.36B + 0.57C - 0.56AB - 0.62\,A\,C + 0.095BC - 3.67\,A^2 - 3.88B^2 - 3.28C^2], \quad (13b)$$

where A, B, and C are the coded values of activating agent (H_3PO_4 and KOH) concentration, activation temperature, and activation time, respectively.

3.4. The Adsorption Capacity of the Modified Biosorbent. The adsorbent was prepared from *Teff* straw using chemical

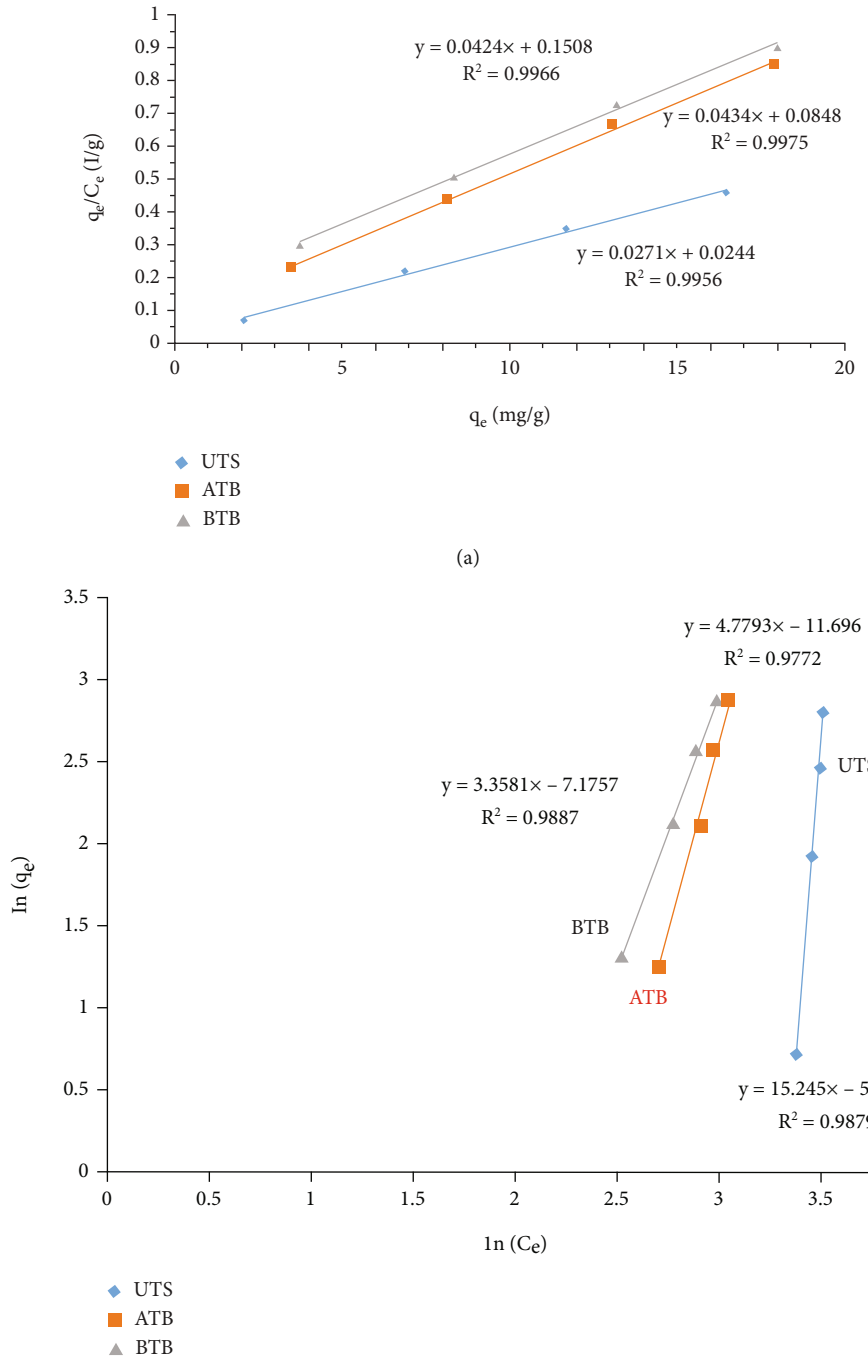

Figure 9: Linear fitting for adsorption of Cr (VI) metal ion: (a) Langmuir isotherm and (b) Freundlich isotherm.

activating agents: H_3PO_4 which acts as the most common acid activating agent for synthesis of biosorbent due to high carbon yield, ease of acid recovery, and low operation time and KOH which acts as a primary activating agent that creates a high specific surface area in the preparation of biosorbent [31, 35]. The adsorption capacity of *Teff* straw-based biosorbent was investigated by analyzing adsorption parameters of adsorbent dosage, initial Cr (VI) concentration, contact time, and temperature effect on the prepared biosorbent.

3.4.1. Effect of Adsorbent Dosage on Adsorption Capacity. The effect of biosorbent dose on the removal efficiency of Cr (VI) metal ion was examined by varying the quantity of biosorbents from 0.5 to 3 g by keeping other parameters constant at a contact time of 4 h, pH of 2, initial Cr (VI) concentration of 100 mg/L, and agitation speed of 150 rpm. Percentage Cr (VI) removal increased with increasing biosorbent dosage (Figure 8(a)) due to increased adsorptive surface area, and the availability of more active sites on the adsorbent

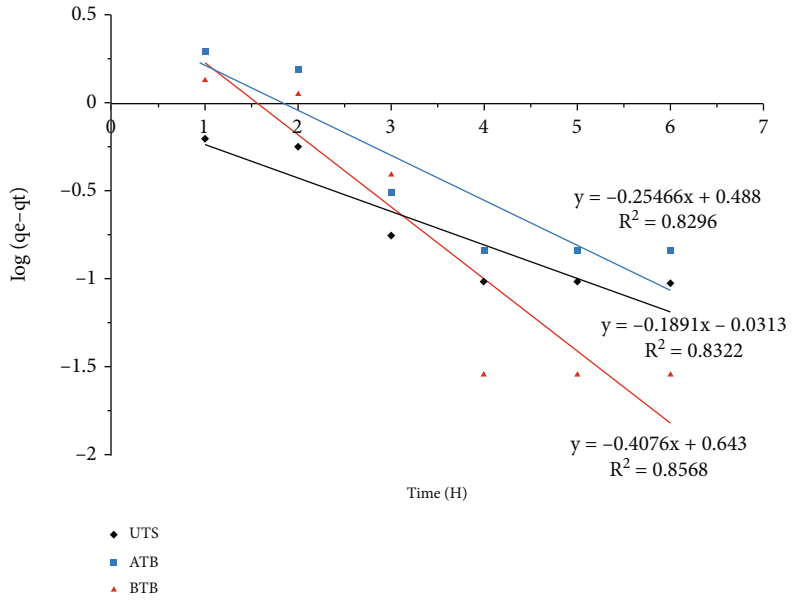

(a)

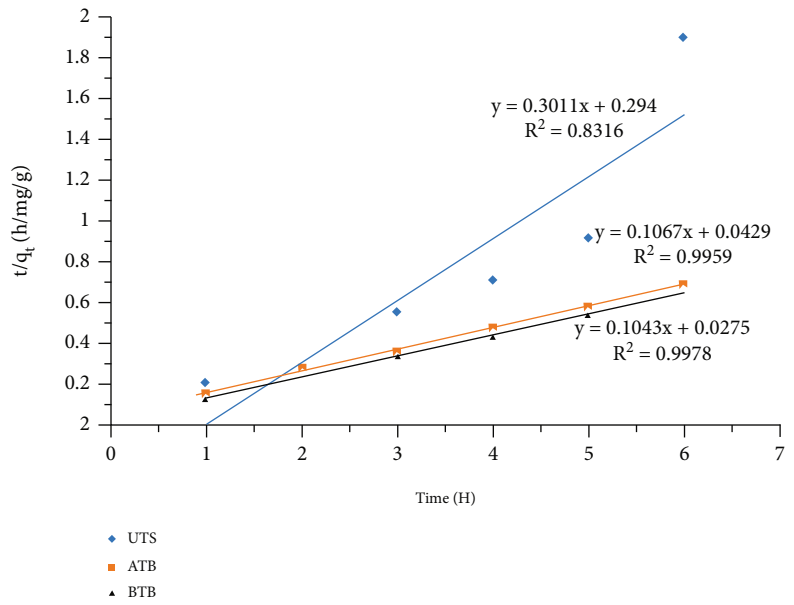

(b)

Figure 10: Continued.

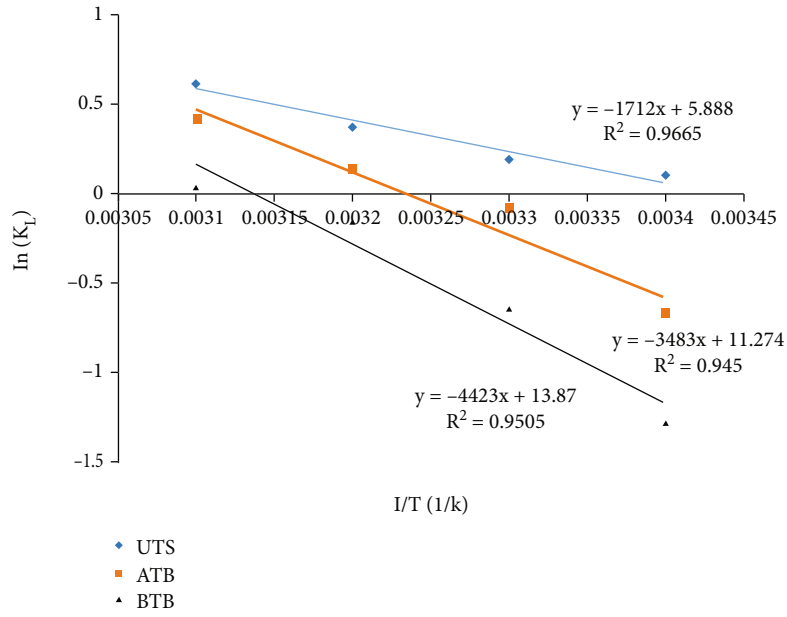

(c)

Figure 10: Plots of Cr (VI) adsorption onto *Teff* straw biosorbent: (a) pseudo-first order and (b) pseudo-second order and (c) Van't Hoff's plot.

Table 4: Thermodynamic parameters for adsorption of Cr (VI) onto *Teff* straw biosorbent.

Biosorbent	T (K)	K_L (L/mg)	ΔG^o (KJmol^{-1})	ΔH^o (KJmol^{-1})	ΔS^o (JK^{-1}mol^{-1})	R^2
UTS	298	1.11	-0.258	14.234	48.953	0.9665
	303	1.22	-0.501			
	313	1.46	-0.984			
	323	1.85	-1.652			
ATB	298	0.512	1.660	28.958	93.732	0.945
	303	0.93	0.184			
	313	1.15	-0.364			
	323	1.52	-1.128			
BTB	298	0.28	3.154	36.773	115.315	0.9505
	303	0.53	1.60			
	313	0.86	0.393			
	323	1.04	-0.110			

surface until the equilibrium point was reached. However, beyond equilibrium, all active sites of the biosorbent were fully occupied by Cr (VI) metal ions, i.e., totally no active binding sites to accumulate extra metal ions, which is no significant increase in percentage removal of Cr (VI). Figure 8(a) shows that the maximum percentage Cr (VI) metal ion removal was attained around 1 g. Optimum *Teff* straw biosorbent dosage was 47%, 83.1%, and 89.3% for UTS, ATB, and BTB, respectively. The Cr (VI) removal percentage increased from 35% to 47%, 63 to 83.1%, and 72 to 89.3% as the biosorbent quantity increased from 0.5 to 3 g at room temperature (25°C).

3.4.2. Effect of Initial Cr (VI) Concentration on Adsorption Capacity. Mainly, the biosorption of metal ions depends on the available binding active sites of the biosorbent. Figure 8(b) shows the influence of initial Cr (VI) concentration on the metal ion biosorption. The removal efficiency decreased by keeping other parameters constant and varying, the Cr (VI) concentration 50 to 200 mg/L.

3.4.3. Effect of Temperature on the Adsorption of Cr (VI) Metal Ions. The temperature has a significant effect on the adsorption of heavy metals onto the prepared biosorbent. This effect is because the pollutants might be soluble at given temperatures. Thus, the experiments were conducted magnetically at different temperatures (25, 30, 40, and 50°C) in the present study. Figure 8(c) shows that as the temperature increased, the percentage removal of Cr (VI) ions decreased from 92% at 25°C to 85% at 50°C. The

Table 5: Summary of literature values for adsorption of metal ions using various biosorbent sources.

Biosorbent sources	Adsorbate	Optimum adsorption parameters	Biosorption capacity	Main findings of the research	Reference
Banana peel	Cr (VI)	pH = 5.5, time = 60 min	1.41 mg/g	Langmuir and Freundlich's model better fitted experimental data, and pseudo-second order was more fitted than pseudo-first-order kinetics.	Boeykens et al. (2018)
Wheat bran	Pb^{+2}	pH = 5.5, time = 60 min	24.70 mg/g	Langmuir and Freundlich's model better fitted experimental data, and pseudo-second order was more fitted than pseudo-first-order kinetics.	Boeykens et al. (2018)
Nirmali seed	Cr (VI)	—	59.00 mg/g	Langmuir model better fitted experimental data, and pseudo-second order were more fitted than pseudo-first order kinetics.	Lakshmipathiraj and Umamaheswari (2014)
Canola meal	Cd^{+2}	Adsorbent dose = 4.0 g/L and pH = 5.0	2.07 mg/g	Dubinin-Radushkevich>Freundlich > Langmuir > Sips > Temkin for linear models, and pseudo-second order was more fitted than pseudo-first-order kinetics.	Gonçalves et al. [42]
Tobacco	Cd^{+2}	Adsorbent dose = 4.0 g/L and pH = 3.0 to 7.0	—	The occurrence of Cd^{2+} chemisorption and physisorption in mono- and multilayers was revealed with the goodness of the Langmuir, Freundlich, Dubinin-Radushkevich, Sips, and Temkin models; and the excellent fit for pseudo-first-order and pseudo-second-order kinetics shows intraparticle diffusion.	Manfrin et al. [43]
Canola meal	Pb^{+2}	140 min contact time	80% using H_2SO_4 modification	Langmuir model fitted better and predominance of chemisorption (pseudo-second-order kinetics).	Gonçalves et al. [42]
Crambe biomass	Zn^{+2}	—	72% for H_2O_2, 22% H_2SO_4, and 80% for NaOH modification	Occurrence of mono and multilayer adsorption of Zn^{+2}.	Schwantes et al. [44]
Grape stem waste	Cd^{+2}	4.591 for H_2O_2, 2.88 for H_2SO_4, and 14.92 for NaOH	66% for NaOH, 33% for H_2O_2, and 8.3% for H_2SO_4 modifications	Langmuir's model better fitted experimental data and pseudo-second-order kinetics fit better than pseudo-first-order kinetics.	Schwantes et al. [45]
Açaí endocarp	Cd^{2+}, Pb^{2+} and Cr^{3+}	pH = 6.0, 5.0, and 4.0, biosorbent dose = 8, 20, and 12 g/L for Cd^{2+}, Pb^{2+}, and Cr^{3+}, respectively, and 1 h contact time	1.17, 0.49, and 0.49 mg/g for Cd^{2+}, Pb^{2+}, and Cr^{3+}, respectively	Langmuir's model had the best fit for $Cd^{2+}$and Cr^{3+} and Freundlich's model exhibited the best fit for Pb^{2+} and best fit by the pseudo-second-order model kinetics, from the thermodynamic analysis spontaneous and endothermic process for Cd^{2+} and Pb^{2+} ion adsorption.	Gonçalves et al. [46]
Jatropha curcas L.	Cr^{3+}	pH = 5.5, adsorbent dose = 8 g/L, within 60 min time	22.88 mg/g	Langmuir's model was well fitted, with the occurrence of chemosorption in mono- and multilayers.	Gonçalves et al. [47]
Jatropha curcas L.	Cd^{2+},	pH = 5.5, adsorbent dose = 8 g/L, within 60 min time	34.67 mg/g	Langmuir's model better fitted experimental data with the dominance of chemosorption in monolayers.	Nacke et al. [48]

Table 5: Continued.

Biosorbent sources	Adsorbate	Optimum adsorption parameters	Biosorption capacity	Main findings of the research	Reference
Teff straw	Cr (VI)	pH = 2 and adsorbent dose = 0.6 g	3.51 mg/g	The Langmuir model was very well fitted than the Freundlich model; pseudo-second order was more fitted than pseudo-first-order kinetics.	Tadesse et al. [18]
Teff straw	Cr (VI)	Initial Cr (VI) = 75 mg/L, adsorbent dose = 1.0 g, and adsorbent dose = 2.0 g for ATB and BTB, respectively	83.1% for ATB and 89.3% for BTB modification	The Langmuir model is well fitted compared to the Freundlich model, and pseudo-second order is more fitted than pseudo-first-order kinetics. The thermodynamic analysis showed the spontaneous and endothermic process for Cr (VI) ion adsorption.	This study

main reason for the adverse effect of temperature on percentage adsorption has been that a higher temperature destroys the binding sites on the biosorbent. Thus, increasing temperature favors adverse effects for the adsorption of aqueous chromium ions [35, 39].

3.5. Adsorption Isotherm Studies. To analyze the isotherms data, the Langmuir and Freundlich equilibrium models were the most common and familiar models. The Langmuir isotherm assumes that the adsorbent forms monolayer coverage, and adsorption takes place at the specific surface of the adsorbent with no lateral interaction between the sorbed molecules, whereas the Freundlich isotherm model adsorption takes place on heterogeneous surface (multilayer adsorption). The most appropriate correlation of the equilibrium data was examined by taking various initial concentration values, C_o of Cr (VI) (50-200 mg/L). The Langmuir isotherm characteristics can be elaborated by the dimensionless constant that is the separation factor (R_L). In this study, the value of R_L was obtained to be 0.009, 0.020, and 0.034 for UTS, ATB, and BTB, respectively. The results indicate that the adsorption of Cr (VI) onto *Teff* straw biosorbent was favorable because of ($0 < R_L < 1$) [23]. Therefore, R^2 values from Table 3 shows that the Langmuir isotherm gave better fitting than the Freundlich isotherm. Figures 9(a) and 9(b) show the linear fitting of the Langmuir isotherm and linear fitting of the Freundlich isotherm models for the adsorption of Cr (VI), respectively.

3.6. Adsorption Kinetic Studies. The prediction of kinetic variables has given important data about designing and modeling of adsorption process as well as used to select the optimized conditions of a batch process. Adsorption experiments were conducted to investigate the behavior of *Teff* straw biosorbent and to determine the rate-controlling mechanism of the biosorption of Cr (VI) ions onto *Teff* straw biomass. In the present study, pseudo-first-order and pseudo-second-order kinetic models were applied to scrutinize the nature and pathway of Cr (VI) adsorption on Teff straw-based biosorbent. First contact time effect on adsorption was investigated by varying soaking time from 1 to 6 h in 100 mg/L of Cr (VI) of 100 mL solution transferred into 1 g chemically activated biosorbent in 250 mL conical flask.

As shown in Figure 8(d), the amount of adsorbed q_t (mg/g) increased with the increased contact time until it reached the optimum value. It also clearly shows that the initial adsorption rate was rapid, which is due to the availability of high vacant binding sites of the biosorbent for the adsorption, and then slowly increased because of the saturation of the active sites for the biosorbent until it reached equilibrium at ~4 h of contact time. However, after a maximum point, the biosorption capacity of *Teff* straw tends to decline whenever contact time continues because of the instability binding of Cr (VI) by biosorbent so that Cr (VI), which was initially adsorbed by the biosorbent, would detach as introduced by Alif and Khairat, Andas et al., and Overah [30, 40, 41]. The adsorption equilibrium data were then analyzed using pseudo-first-order and pseudo-second-order models in the present study. q_e, k_1, k_2, and respective R^2 for each type of biosorbent can be obtained from the slope and intercept of Figures 10(a) and 10(b).

As shown in Table 3, the pseudo-second-order model was fitted with the experimental data compared to the pseudo-first-order model, as confirmed by higher correlation coefficient values, R^2. Thus, the calculated value of q_e (3.32, 9.40, and 9.60 mg/g of UTS, ATB, and BTB, respectively) obtained from the pseudo-second-order plot agrees with some extent to the experimental values (5.60, 8.82, and 9.23 mg/g). Thus, the primary rate-determining step is the adsorption rate of pseudo-second-order that relies on the chemisorption or chemical adsorption.

3.7. Adsorption Thermodynamics. Adsorption thermodynamics were determined using thermodynamic parameters (viz., change in free energy, ΔG^o; change in enthalpy, ΔH^o; and change in entropy ΔS^o) conducted at various temperatures (25, 30, 40, and 50°C). The parameters can be found in Van't Hoff's plot (Figure 10(c)).

Table 4 indicates the calculated values of thermodynamic parameters investigated in this study as follows: change in enthalpy, ΔH^o = +14.234, +28.958,+36.773 KJ/mol and change in entropy, ΔS^o = +48.953, +93.732,+115.315 J/K.mol of UTS, ATB, and BTB, respectively. The positive enthalpy values indicated that the adsorption of Cr (VI) onto *Teff* straw is an endothermic process. The positive entropy values also implied an increase in the degree of

randomness at the solid-solution interface during adsorption progress. The negative values ΔG^o indicate that Cr (VI) adsorption is a spontaneous and favorable process.

3.8. Comparison of the Obtained Adsorption Parameters with the Literature Values. Various researchers have shown that adsorbents obtained from various agricultural wastes have been widely used to remove different toxic heavy metals from wastewater. For example, Tadesse et al. [18] have reported *Teff* straw as a potential low-cost material for removing Cr (VI) from aqueous samples. The maximum Cr (VI) adsorption capacity of 3.51 mg/g was obtained at initial pH of 2.0 and an adsorbent dose of 0.6 g. The results of their adsorption study showed that the Langmuir model was found to fit better to the Freundlich model and pseudo-second order was found to fit as compared to pseudo-first-order kinetics. Gonçalves et al. [42] have studied the adsorption of Pb^{+2} ions from canola meal using H_2SO_4 modification. Their study revealed that the removal efficiency of 80% Pb^{+2} ions was obtained at 140 min contact time. The adsorption model study also showed that the Langmuir model was found to fit better to the Freundlich model and pseudo-second order was found to fit as compared to pseudo-first-order kinetics. Similar results with this study were obtained in the present study with acid- and base-treated *Teff* straw biomass. Table 5 summarizes the results of various literature for adsorption of different metal ions using various biomass sources. The results of the present investigation are well competent compared to the reported values with some alleviate. The adsorption capacity varies and depends on the individual adsorbent's characteristics, the adsorbate's initial concentration, and the extent of surface modification. It is to be noted that *Teff* straw could be considered as one of the potential low-cost, local availability, and environmentally friend adsorbent materials to be used reliably for the efficient removal of toxic metals, such as Cr (VI), from contaminated wastewater.

4. Conclusion

The chemically modified *Teff* straw-based biosorbent exhibited effective Cr (VI) metal ion removal efficiency from aqueous solution due to the availability of active binding sites on the surface of the modified biomass.

The effect of concentration of activating agents (H_3PO_4 and KOH), activation temperature, and activation time on Cr (VI) removal efficiency of chemically modified *Teff* straw biosorbent was better described by quadratic polynomial model adequately. The good agreement between experimental and predicted values was revealed from the analysis of variance outputs.

The characterization showed that the *Teff* straw biosorbent has good properties compared with other biomass source biosorbents. The optimum values for maximum Cr (VI) removal efficiency 92.5% of 2 M, 110°C, and 4 h of activating agent (H_3PO_4) concentration, activation temperature, and activation time, respectively, were obtained by using acid-treated *Teff* straw biosorbent (ATB). Similarly, the optimum values for maximum Cr (VI) removal efficiency of 95.2% under this study was as follows: 1.5 M, 105°C, and 3.5 h of activating agent (KOH) concentration, activation temperature, and activation time, respectively, by using base-treated *Teff* straw biosorbent (BTB).

The isotherms exhibited the Langmuir behavior at all temperatures, which indicates that adsorption took place via monolayer surface binding. The adsorption kinetic data agreed with the pseudo-second-order kinetic model for untreated and chemically modified *Teff* straw biosorbent. Furthermore, based on thermodynamic parameters, the adsorption of Cr (VI) onto untreated and chemically modified *Teff* straw biosorbent was a spontaneous and endothermic process.

Abbreviations

α:	Initial adsorption rate (mg g^{-1} min)
ΔH^o:	Standard enthalpy change (kJ/mol)
β:	The extent of surface coverage (g/mg)
λ:	Wavelength
ΔG^o:	Standard free energy change (kJ/mol)
ΔS^o:	Standard entropy change (kJ/mol)
ATB:	Acid-treated biosorbent
BBD:	Box-Behnken design
BTB:	Base-treated biosorbent
C_e:	Metal ion concertation at equilibrium (mg/L)
C_o:	The initial concentration of metal ion (mg/L)
-COOH:	Carboxyl functional group
Cr (VI) or Cr^{6+}:	Hexavalent chromium ion
DPC:	1,5-Diphenylcarbazide
DTG:	Differential thermogravimetric analysis
FTIR:	Fourier transform infrared spectroscopy
H_2SO_4:	Sulphuric acid
H_3PO_4:	Phosphoric acid
K_1:	The rate constant for pseudo-first-order kinetics (min^{-1})
K_2:	The rate constant for pseudo-second-order kinetics (g mg^{-1} min^{-1})
$K_2Cr_2O_7$:	Potassium dichromate
K_F:	The Freundlich constant (L/g)
K_L:	The Langmuir equilibrium constant (L/g)
KOH:	Potassium hydroxide
K_T:	Tempkin equilibrium constant (L/g)
M:	Molarity
MB:	Methylene blue
N:	The Freundlich exponent (g/L)
NaOH:	Sodium hydroxide
-OH:	Hydroxyl ion functional group
pH:	Hydrogen/hydronium ion concentration
q_e:	Amount of adsorbed at equilibrium (mg/g)
q_m:	The theoretical monolayer saturation capacity
q_t:	Amount of adsorbed at any time (mg/g)
R:	Universal gas constant (8.314 J/mol-K)
RSM:	Response surface methodology
SEM:	Scanning electron microscope

Si-OH: Silanol functional group
TGA: Thermogravimetric analysis
UTS: Untreated *Teff* straw
UV: Ultraviolet
W: Watt
XRD: X-ray diffraction spectroscopy.

Data Availability

The datasets generated during and/or analyzed during the current study are available from the corresponding author on reasonable request.

Conflicts of Interest

The authors declare that they have no conflicts of interest.

Acknowledgments

The first author acknowledges the Defence University College of Engineering, Ethiopia, for providing experimentation support to do the research.

References

[1] S. Basharat, R. Rehman, and L. Mitu, "Adsorptive separation of brilliant green dye from water by tartaric acid-treated holarrhena antidysenterica and Citrullus colocynthis biowaste," *Journal of Chemistry*, vol. 2021, no. 8, 2021.

[2] M. A. Yahya, M. H. Mansor, W. A. Zolkarnaini et al., "A brief review on activated carbon derived from agriculture by-product," *AIP Conference Proceedings*, , no. 1, article 030023, 2018.

[3] J. Bedia, M. Peñas-Garzón, A. Gómez-Avilés, J. J. Rodriguez, and C. Belver, "A review on the synthesis and characterization of biomass-derived carbons for adsorption of emerging contaminants from water," *C*, vol. 4, no. 4, p. 63, 2018.

[4] Z. Z. Chowdhury, S. B. Abd Hamid, R. Das et al., "Preparation of carbonaceous adsorbents from lignocellulosic biomass and their use in removal of contaminants from aqueous solution," *Bio Resources*, vol. 8, no. 4, pp. 6523–6555, 2013.

[5] P. C. Lindholm-Lehto, "Biosorption of heavy metals by lignocellulosic biomass and chemical analysis," *Bio Resources*, vol. 14, no. 2, pp. 4952–4995, 2019.

[6] S. A. Olawale, "Biosorption of heavy metals: a mini review," *Acta Scientific Agriculture*, vol. 3, no. 2, pp. 22–25, 2019.

[7] S. Darmawan, N. J. Wistara, G. Pari, A. Maddu, and W. Syafii, "Characterization of lignocellulosic biomass as raw material for the production of porous carbon-based materials," *Bio Resources*, vol. 11, no. 2, pp. 3561–3574, 2016.

[8] A. Seyoum and L. Asso, *Heavy Metals Removal from Electroplating Waste Water Using Activated Carbon of Coffee Husk*, T. Aragaw, Ed., Center for Environmental Science Prese, 2015, A thesis Submitted to.

[9] C. Vargas, P. F. Brandão, J. Ágreda, and E. Castillo, "Bioadsorption using compost: an alternative for removal of chromium (VI) from aqueous solutions," *Bio Resources*, vol. 7, no. 3, pp. 2711–2727, 2012.

[10] K. Le Van and T. T. L. Thi, "Activated carbon derived from rice husk by NaOH activation and its application in supercapacitor," *Progress in Natural Science: Materials International*, vol. 24, no. 3, pp. 191–198, 2014.

[11] J. Febrianto, A. N. Kosasih, J. Sunarso, Y. H. Ju, N. Indraswati, and S. Ismadji, "Equilibrium and kinetic studies in adsorption of heavy metals using biosorbent: a summary of recent studies," *Journal of Hazardous Materials*, vol. 162, no. 2-3, pp. 616–645, 2009.

[12] V. O. Shikuku, F. F. Donato, C. O. Kowenje, R. Zanella, and O. D. Prestes, "A comparison of adsorption equilibrium, kinetics and thermodynamics of aqueous phase clomazone between faujasite X and a natural zeolite from Kenya," *South African Journal of Chemistry*, vol. 68, pp. 245–252, 2015.

[13] J. A. Fernández-López, J. M. Angosto, and M. D. Avilés, "Biosorption of hexavalent chromium from aqueous medium with opuntia biomass," *The Scientific World Journal*, vol. 2014, 8 pages, 2014.

[14] A. Ghosh, P. Das, and K. Sinha, "Modeling of biosorption of Cu (II) by alkali-modified spent tea leaves using response surface methodology (RSM) and artificial neural network (ANN)," *Applied Water Science*, vol. 5, no. 2, pp. 191–199, 2015.

[15] J. Sahira, A. Mandira, P. B. Prasad, and P. R. Ram, "Effects of activating agents on the activated carbons prepared from lapsi seed stone," *Research Journal of Chemical Sciences*, vol. 2231, p. 606X, 2013.

[16] T. Subramani and S. Sindhu, "Batch study experiments and column analysis for finding out a suitable biosorbent for the removal of heavy metals from electroplating industry effluent," *International journal of engineering research and applications*, vol. 2, no. 4, pp. 172–184, 2012.

[17] M. Sen and M. G. Dastidar, "Chromium removal using various biosorbents," *Journal of Environmental Health Science & Engineering*, vol. 7, no. 3, pp. 182–190, 2010.

[18] B. Tadesse, E. Teju, and N. Megersa, "The Teff straw: a novel low-cost adsorbent for quantitative removal of Cr (VI) from contaminated aqueous samples," *Desalination and Water Treatment*, vol. 56, no. 11, pp. 2925–2936, 2014.

[19] C. Tejada-Tovar, A. González-Delgado, and A. Villabona-Ortíz, "Comparison of banana peel biosorbents for the removal of Cr (VI) from water," *Contemporary Engineering Sciences*, vol. 11, no. 21, pp. 1033–1041, 2018.

[20] R. Weideman, E. Fosso-Kankeu, D. Moyakhe, F. B. Waanders, M. Le Roux, and Q. P. Campbell, "Hydrothermal preparation of biochar from spent coffee grounds, and its application for the removal of cadmium from coal tailings leachate," *Journal of the Southern African Institute of Mining and Metallurgy*, vol. 119, no. 7, pp. 607–612, 2019.

[21] A. A. Tesfaw and B. Z. Tizazu, "Reducing sugar production from teff straw biomass using dilute sulfuric acid hydrolysis: characterization and optimization using response surface methodology," *International Journal of Biomaterials*, vol. 2021, Article ID 2857764, 2021.

[22] A. B. Wassie and V. C. Srivastava, "Teff straw characterization and utilization for chromium removal from wastewater: kinetics, isotherm and thermodynamic modelling," *Journal of Environmental Chemical Engineering*, vol. 4, no. 1, pp. 1117–1125, 2016.

[23] A. B. Wassie and V. C. Srivastava, "Chemical treatment of teff straw by sodium hydroxide, phosphoric acid and zinc chloride: adsorptive removal of chromium," *International journal of Environmental Science and Technology*, vol. 13, no. 10, pp. 2415–2426, 2016.

[24] E. K. Doboy, H. Z. Adjia, R. Kamga, and F. Lorraine, "Production and Characterization of Rice Husk Biosorbent from Far

North Cameroon," *Environment and Pollution*, vol. 8, pp. 1–7, 2019.

[25] S. Bahaa, I. A. Al-Baldawi, S. R. Yaseen, and S. R. S. Abdullah, "Biosorption of heavy metals from synthetic wastewater by using macro algae collected from Iraqi Marshlands," *Journal of Ecological Engineering*, vol. 20, no. 11, pp. 18–22, 2019.

[26] B. Z. Tizazu and V. S. Moholkar, "Kinetic and thermodynamic analysis of dilute acid hydrolysis of sugarcane bagasse," *Bioresource Technology*, vol. 250, pp. 197–203, 2018.

[27] S. H. Abbas, I. M. Ismail, T. M. Mostafa, and A. H. Sulaymon, "Biosorption of heavy metals: a review," *Journal of Chemical Science and Technology*, vol. 3, no. 4, pp. 74–102, 2014.

[28] O. A. Adeeyo, O. M. Oresegun, and T. E. Oladimeji, "Compositional analysis of lignocellulosic materials: evaluation of an economically viable method suitable for woody and non-woody biomass," *American Journal of Engineering Research (AJER)*, vol. 4, no. 4, pp. 14–19, 2015.

[29] R. Shokoohi, M. Saghi, H. Ghafari, and M. Hadi, "Biosorption of iron from aqueous solution by dried biomass of activated sludge," *Journal of Environmental Health Science & Engineering*, vol. 6, no. 2, pp. 107–114, 2009.

[30] L. C. Overah, "Biosorption of Cr (III) from aqueous solution by the leaf biomass of Calotropis procera–'Bom bom," *Journal of Applied Sciences and Environmental Management*, vol. 15, no. 1, 2011.

[31] F. T. Ademiluyi and E. O. David-West, "Effect of chemical activation on the adsorption of heavy metals using activated carbons from waste materials," *International Scholarly Research Notices*, vol. 2012, Article ID 674209, 2012.

[32] P. C. Emenike, D. O. Omole, B. U. Ngene, and I. T. Tenebe, "*Potentiality of Agricultural Adsorbent for the Sequestering of Metal Ions from Wastewater*," *Global Journal Environment Science Management*, vol. 2, no. 4, pp. 411–442, 2016.

[33] O. K. Ince and I. N. C. E. Muharrem, "An overview of adsorption technique for heavy metal removal from water/wastewater: a critical review," *International Journal of Pure and Applied Sciences*, vol. 3, no. 2, pp. 10–19, 2017.

[34] M. S. Islam, M. A. Rouf, S. Fujimoto, and T. Minowa, "Preparation and characterization of activated carbon from bio-diesel by-products (Jatropha seedcake) by steam activation," *Bangladesh Journal of Scientific and Industrial Research*, vol. 47, no. 3, pp. 257–264, 2012.

[35] S. Lou, "Applied adsorption kinetics model for removal of hazards from aqueous solution: more informational parameters for industrial design," *Journal of Environmental Science and Public Health*, vol. 1, no. 4, pp. 228–239, 2017.

[36] T. A. M. Msagati, O. F. Olorundare, R. W. M. Krause, J. O. Okonkwo, and B. B. Mamba, "Activated carbon from lignocellulosic waste residues: effect of activating agent on porosity characteristics and use as adsorbents for organic species," *Water, Air, & Soil Pollution*, vol. 225, no. 3, pp. 1–14, 2014.

[37] X. Li, F. Yang, P. Li et al., "Optimization of preparation process of activated carbon from chestnut burs assisted by microwave and pore structural characterization analysis," *Journal of the Air & Waste Management Association*, vol. 65, no. 11, pp. 1297–1305, 2015.

[38] N. H. Shalaby, E. M. Ewais, R. M. Elsaadany, and A. Ahmed, "Rice husk templated water treatment sludge as low cost dye and metal adsorbent," *Egyptian Journal of Petroleum*, vol. 26, no. 3, pp. 661–668, 2017.

[39] N. Hussain, S. Chantrapromma, T. Suwunwong, and K. Phoungthong, "Cadmium (II) removal from aqueous solution using magnetic spent coffee ground biochar: Kinetics, isotherm and thermodynamic adsorption," *Materials Research Express*, vol. 7, no. 8, p. 085503, 2017.

[40] A. Alif and K. Mutiara, "Optimization of biosorption process copper using cuttlefish shell (Sepia recurvirostra) in water solution," *Der Pharma Chemica*, vol. 8, no. 10, pp. 236–242, 2016.

[41] J. Andas, M. L. A. Rahman, and M. S. M. Yahya, "Preparation and characterization of activated carbon from palm kernel shell," in *IOP Conference Series: Materials Science and Engineering (Vol. 226, No. 1, p. 012156)*, IOP Publishing, 2017.

[42] A. C. Gonçalves, D. Schwantes, A. L. Braccini, F. Albornoz, É. Conradi Jr., and J. Zimmermann, "Canola meal-derived activated biochar treated with NaOH and CO2 as an effective tool for Cd removal," *Journal of Chemical Technology & Biotechnology*, vol. 97, no. 1, pp. 87–100, 2021.

[43] J. Manfrin, A. C. Gonçalves Junior, D. Schwantes, J. Zimmermann, and E. Conradi Junior, "Effective Cd2+ removal from water using novel micro-mesoporous activated carbons obtained from tobacco: CCD approach, optimization, kinetic, and isotherm studies," *Journal of Environmental Health Science and Engineering*, vol. 19, no. 2, pp. 1851–1874, 2021.

[44] D. Schwantes, A. C. Gonçalves Jr., A. da Paz Schiller, J. Manfrin, L. A. V. Bianco, and A. G. Rosenberger, "Eco-friendly, renewable Crambe abyssinica Hochst-based adsorbents remove high quantities of Zn 2+ in water," *Journal of Environmental Health Science and Engineering*, vol. 18, no. 2, pp. 809–823, 2020.

[45] D. Schwantes, A. C. Gonçalves, A. De Varennes, and A. L. Braccini, "Modified grape stem as a renewable adsorbent for cadmium removal," *Water Science and Technology*, vol. 78, no. 11, pp. 2308–2320, 2018.

[46] A. C. Gonçalves, D. Schwantes, M. A. Campagnolo, D. C. Dragunski, C. R. T. Tarley, and A. K. D. S. Silva, "Removal of toxic metals using endocarp of açaí berry as biosorbent," *Water Science and Technology*, vol. 77, no. 6, pp. 1547–1557, 2018.

[47] A. C. Gonçalves, H. Nacke, D. Schwantes et al., "Adsorption mechanism of chromium (III) using biosorbents of Jatropha curcas L," *Environmental Science and Pollution Research*, vol. 24, no. 27, pp. 21778–21790, 2017.

[48] H. Nacke, A. C. Gonçalves, G. F. Coelho et al., "Removal of Cd (II) from water using the waste of jatropha fruit (Jatropha curcas L.)," *Applied Water Science*, vol. 7, no. 6, pp. 3207–3222, 2017.

[49] N. Benderdouche, B. Bestani, and M. Hamzaoui, "The use of linear and nonlinear methods for adsorption isotherm optimization of basic green 4-dye onto sawdust-based activated carbon," *Journal of Material Environmental Science*, vol. 9, no. 4, pp. 1110–1118, 2018.

[50] A. M. Mansora, J. S. Lima, F. N. Anib, H. Hashima, and W. S. Hoa, "Characteristics of cellulose, hemicellulose and lignin of MD2 pineapple biomass," *Chemical Engineer*, vol. 72, no. 1, pp. 79–84, 2019.